Graphical Abstract

To create your abstract, type over the instructions in the template box below.
Fonts or abstract dimensions should not be changed or altered.

Design, synthesis and antibacterial properties of pyrimido[4,5-*b*]indol-8-amine inhibitors of DNA gyrase

Leave this area blank for abstract info.

David H. McGarry[a,*], Ian R. Cooper[a], Rolf Walker[a], Catherine E. Warrilow[a], Mark Pichowicz[a], Andrew J. Ratcliffe[a], Anne-Marie Salisbury[a], Victoria J. Savage[a], Emmanuel Moyo[a], John Maclean[a], Andrew Smith[a], Cédric Charrier[a], Neil R. Stokes[a], David M. Lindsay[b] and William J. Kerr[b]

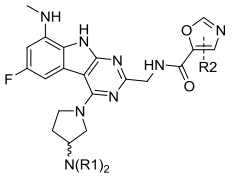

where R1, R2 = H, Me

MIC < 1 µg/mL against gram-positive strains

MIC < 0.25 µg/mL against *M. tuberculosis*

Maintains activity against fluoroquinolone-, isoniazid- and rifampicin-resistant isolates

Bioorganic & Medicinal Chemistry Letters
journal homepage: www.elsevier.com

Design, synthesis and antibacterial properties of pyrimido[4,5-*b*]indol-8-amine inhibitors of DNA gyrase

David H. McGarry[a, *], Ian R. Cooper[a], Rolf Walker[a], Catherine E. Warrilow[a], Mark Pichowicz[a], Andrew J. Ratcliffe[a], Anne-Marie Salisbury[a], Victoria J. Savage[a], Emmanuel Moyo[a], John Maclean[a], Andrew Smith[a], Cédric Charrier[a], Neil R. Stokes[a], David M. Lindsay[b] and William J. Kerr[b]

[a]*Redx Pharma, Alderley Park, Cheshire, SK10 4TG, United Kingdom*
[b]*Department of Pure and Applied Chemistry, University of Strathclyde, WestCHEM, Thomas Graham Building, 295 Cathedral Street, Glasgow, G1 1XL,United Kingdom*

ARTICLE INFO

Article history:
Received
Revised
Accepted
Available online

Keywords:
ESKAPE pathogens
Anti-infectives
Topoisomerases
DNA gyrase
Pyrimido[4,5-*b*]indol-8-amine

ABSTRACT

According to the World Health Organization (WHO), approximately 1.7 million deaths per year are caused by tuberculosis infections. Furthermore, it has been predicted that, by 2050, antibacterial resistance will be the cause of approximately 10 million deaths annually if the issue is not tackled. As a result, novel approaches to treating broad-spectrum bacterial infections are of vital importance. During the course of our wider efforts to discover unique methods of targeting multidrug-resistant (MDR) pathogens, we identified a novel series of amide-linked pyrimido[4,5-*b*]indol-8-amine inhibitors of bacterial type II topoisomerases. Compounds from the series were highly potent against gram-positive bacteria and mycobacteria, with excellent potency being retained against a panel of relevant *Mycobacterium tuberculosis* drug-resistant clinical isolates.

* Corresponding author. e-mail: d.mcgarry@redxpharma.com

Antibiotic resistance is rapidly becoming prevalent in both a clinical and a community setting. Alarmingly, it is predicted that failure to address this issue could lead to approximately 10 million deaths per year by 2050.[1] A recent report by the WHO identified tuberculosis (TB) as a global priority for research and development due to its status as the number one global infectious disease killer, causing 1.7 million deaths per year.[2] A further 12 priority pathogens were identified, consisting of *Acinetobacter baumannii, Pseudomonas aeruginosa, Enterobacteriaceae, Enterococcus faecium, Staphylococcus aureus, Helicobacter pylori, Campylobacter* spp, *Salmonellae, Neisseria gonorrhoeae, Streptococcus pneumoniae, Haemophilus influenzae* and *Shigella* spp.

Antibiotics such as fluoroquinolones have had great clinical success, however, bacteria have evolved resistance to entire classes of antibiotics. Overexpression of efflux pumps, target-specific mutations, modifications to the bacterial cell wall and the generation of drug-inactivating enzymes can all contribute to bacterial resistance.[3] Consequently, research into chemical series' with the ability to target drug-resistant bacteria are of utmost importance. One method of overcoming site-specific mutation resistance is to target alternative binding sites which are capable of inducing the same phenotypic response.

DNA gyrase and topoisomerase IV are two examples of highly homologous bacterial type IIA topoisomerases which have the ability to break, reorganise and religate DNA strands.[4] Without recourse to these enzymes, bacteria are not able to appropriately manipulate the topology of their DNA, resulting in eventual cellular death. Fluoroquinolones target the DNA binding site of topoisomerases in order to elicit their therapeutic effect, however, recent publications have focused on inhibition at an alternative site (the ATPase sites on GyrB/ParE on DNA gyrase/topoisomerase IV respectively) in order to circumvent resistance mechanisms. In the 60 years since the first GyrB/ParE inhibitor, novobiocin **1** (**Figure 1**), was discovered, many chemical series have been developed through fragment-based screening, high-throughput screening and scaffold hopping.[5-10]

Herein we describe the discovery and structure-activity relationship (SAR) of a novel series of amide-linked pyrimido[4,5-*b*]indol-8-amine inhibitors of bacterial type II topoisomerase, which were identified using computational

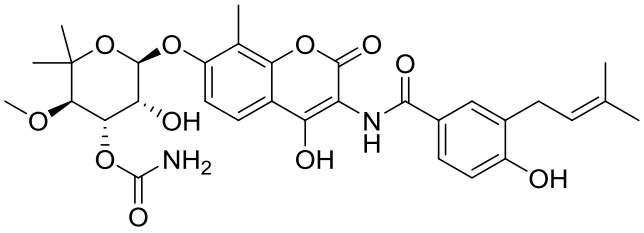

1

Figure 1. Novobiocin **1**

analysis of published GyrB inhibitors and an antibacterial library screen. It was observed in many of the previously published crystal structures of GyrB that a flexible loop adjacent to the ATPase site was poorly ordered, and usually omitted from the deposited coordinates (green arrow, **Figure 2a**). Due to the absence of the resolved loop in many structures, proposed interactions in this area have been poorly modelled computationally. However, when an X-ray crystal structure in which this loop was resolved (PDB: 3G7E, green) was overlayed with a range of inhibitors, an unexplored vector near Asp106 was revealed (blue arrow). It was postulated that establishing initial SAR along this vector could serve to both probe the computational model and allow elaboration of a novel inhibitor series. Investigation of the SAR in this way could afford improvements to a variety of PK properties, by highlighting a region of the scaffold from which further optimisation could progress. In combination with these structural studies, an in-house compound library screen identified hit compound **2aa** (**Figure 2b**, **Table 1**), where the substituent probing the Asp106 vector is attached *via* a novel amide linker. This discovery prompted further investigation of the novel amide-linked pyrimido[4,5-*b*]indol-8-amine scaffold as a means of challenging the SAR in this region.

Utilising the previously reported intermediate **3**[11] (**Scheme 1**) allowed the synthesis of final compounds **2aa-2di** to proceed efficiently *via* a reproducible, reliable route, from which a range of analogues could be generated. Disulfone **3** was identified as an important intermediate, since several points of diversity could be explored from this compound. Substitution with a variety of 3-substituted pyrrolidines yielded compounds **4**, with the relative structural configuration established through an observed Nuclear Overhauser effect between the pyrrolidine substituent and the pyrimidine core (**Scheme 1**).

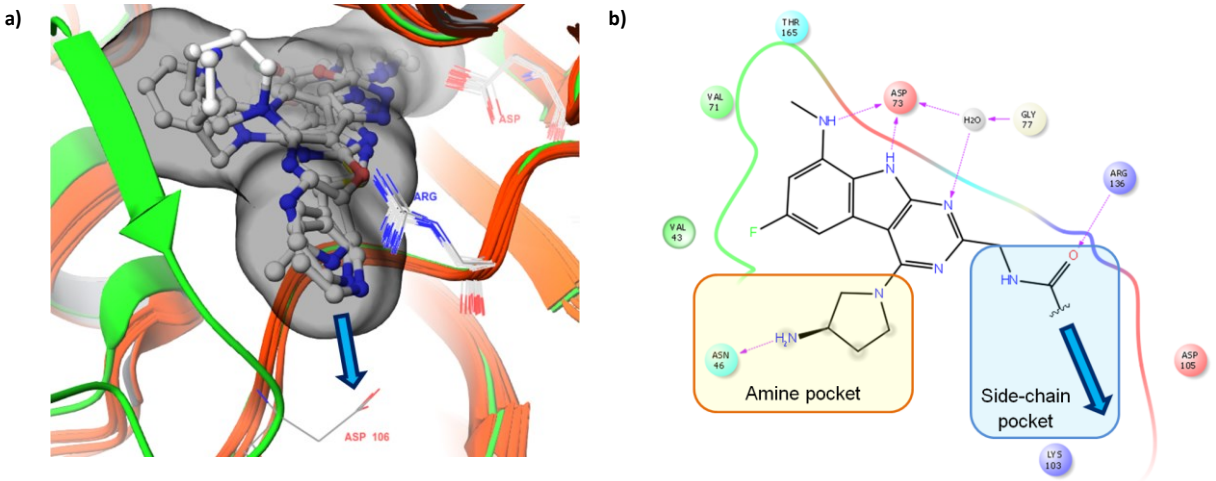

Figure 2. **a**) Proposed vector (blue arrow), from which the inhibitor could be expanded in the side-chain pocket, towards Asp106. Figure generated from overlaying structures of 3G7E,[12] 4K4O[10] and 5D7C.[13] The flexible loop of residues, which are omitted in all structures but present in 3G7E, is highlighted in green. The approximate space-fill surface for the majority of published inhibitors is shown in black. **b**) Hypothesised amide-linked pyrimido[4,5-*b*]indol-8-amine compounds that could utilise a previously underexplored vector (blue arrow). Both figures generated using Maestro Version 10.6.014.[14]

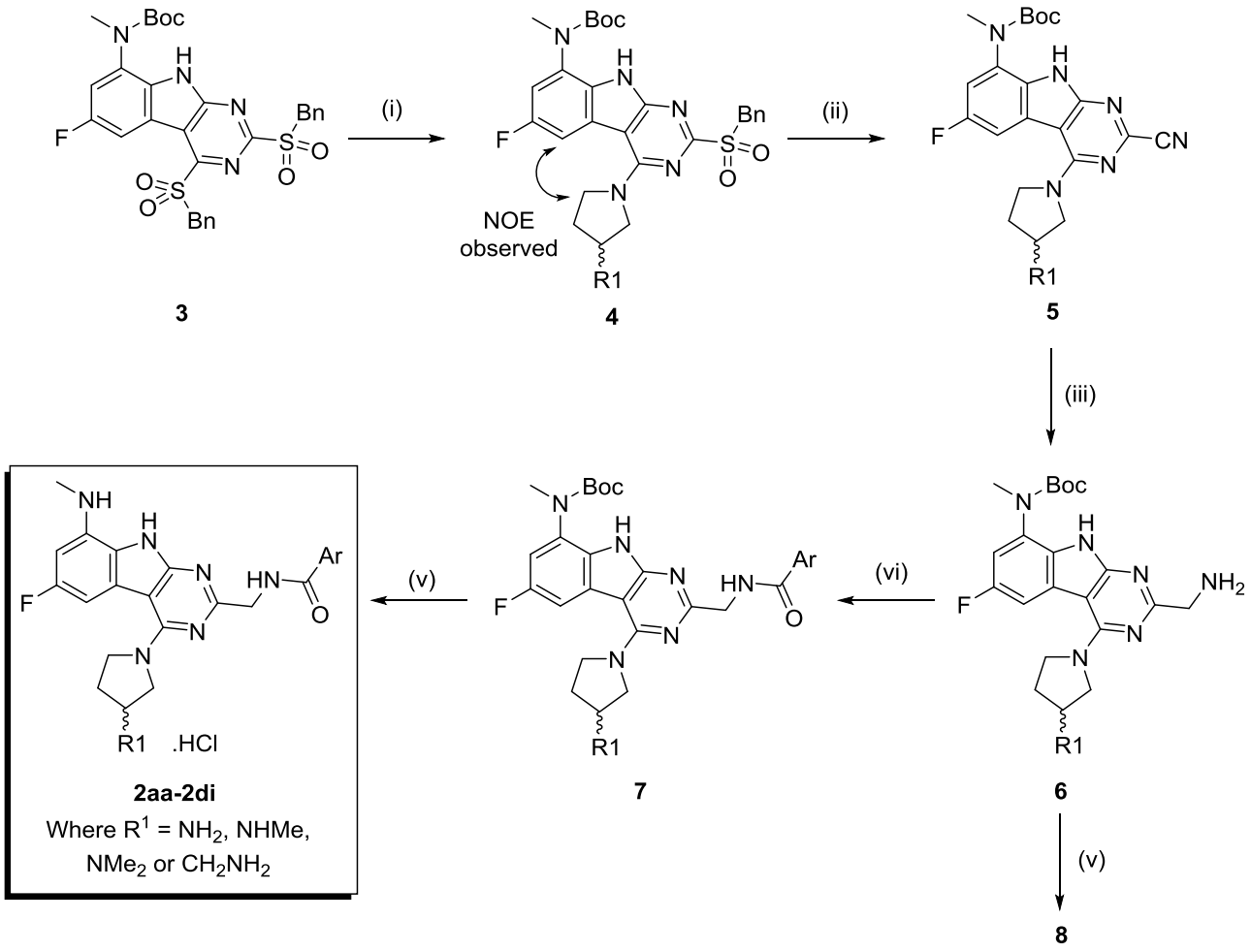

Scheme 1. Use of disulfone **3** to introduce structural diversity. Reagents and conditions: (i) substituted pyrrolidine, K_2CO_3, EtOH, 45 °C, 50 min, MW, 61 - 89% (ii) NaCN, DMF, 100 °C, 16 h, 60 - 89% (iii) Raney nickel, H_2, EtOH, rt, 16 h, 68- 97% (iv) ArCOOH, EDCI, Et_3N, DCM, rt, 16 h, 13 - 67% (v) HCl (4N in dioxane), MeOH, rt, 16 h, 14 - 99%.

Aromatic nucleophilic substitution of **4** with sodium cyanide then afforded key intermediate **5** (**Scheme 1**), which could be elaborated through nitrile reduction, unmasking primary amines of the form **6**. Amide coupling with an appropriate carboxylic acid followed by deprotection yielded amides of the form **2aa-2di** (**Table 1**). The carboxylic acids were selected on the basis of their commercial availability and similarity to those previously reported in the literature.

Final compounds **2aa-2di** were tested against a panel of antibacterial strains (**Table 1**), including gram-positive pathogens (*E. faecalis* and *S. aureus*), gram-negative pathogens (*E. coli*) and mycobacteria (*M. smegmatis* and *M. tuberculosis).*

Incorporation of an oxazole moiety at the amide (**2ac** and **2ad**), provided potency against *M. smegmatis* and *M. tuberculosis* (**Table 1**). Interestingly, a potency increase against gram-positive bacteria and mycobacteria was observed upon *N,N*-dimethylation of the 3-aminopyrrolidine, consistent with the hypothesised increase in permeability upon removal of the H-bond donating ability of the primary/secondary amine. Encouraged by the improved potency of the oxazole subseries, the SAR was further challenged through subsequent methylation of the oxazole ring. Oxazole methylation tended to increase the potency for a series, however, the position of optimal methylation was variable. Computational methods (See **Computational Analysis** section, below) were utilised to aid rationalisation of these results. In order to further profile the series, a selection of compounds were tested against a broader panel of gram-positive and gram-negative bacteria, and assessment of their *in vitro* cytotoxicity was undertaken (**Table 2**).

Representative compounds were found to partially retain activity against a broader spectrum of bacteria, with no toxic effects observed in a HepG2 mammalian cytotoxicity assay for the majority of the tested compounds. Importantly, examples from the series were found to be more potent against *M. tuberculosis* than novobiocin **1**. Target engagement was confirmed by testing for the ability of the inhibitor to prevent DNA supercoiling, and through its capacity to inhibit ATP hydrolysis (**Table 3**). Inhibition of human topoisomerase II decatenation highlighted the high bacterial selectivity of the series (**Table 3**).

As a result of the high potency against *M. tuberculosis*, representative compounds from our novel series were tested against a panel of bacterial strains bearing mechanisms that rendered them resistant to clinically utilised antibiotics. All the resistant strains used were derived from *M. tuberculosis* H37Rv, and carried resistance mechanisms as outlined in **Table 4**.

Gratifyingly, the Redx Pharma series was observed to maintain potency against the tested resistant isolates, highlighting a benefit in the current series compared to the clinically-relevant compounds moxifloxacin, isoniazid, rifampicin and novobiocin.

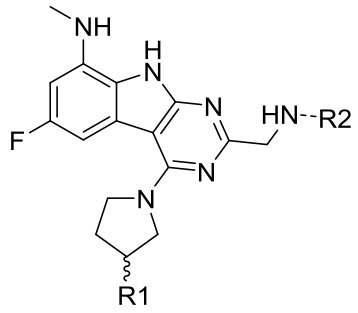

R1							
a =	NH_2	b =	NHMe	c =	NMe_2	d =	CH_2NH_2

R2

a = 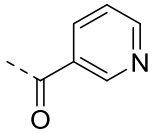

b = 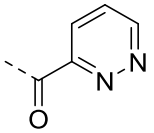

c = 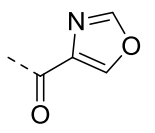

d = 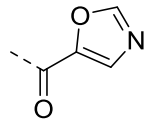

e = 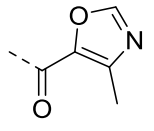

f = 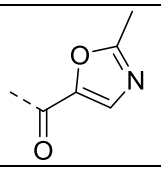

g = 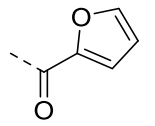

h = 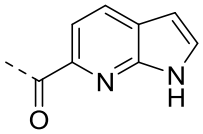

i = 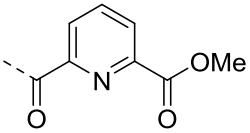

Compound	R1	R2	MIC (μg/mL)[a] Ef	Sa	Ec	Ms	Mt
Novobiocin **1**	-	-	4 (ref.[15])	0.06	>64	1	4 (ref.[16])
8	a	H	8	8	8	N.D.	N.D.
2aa	a	a	0.25	32	8	N.D.	N.D.
2ab	a	b	0.12	8	4	N.D.	N.D.
2ac	a	c	0.06	8	128	0.12	N.D.
2ad	a	d	1	8	4	0.25	0.25
2bc	b	c	0.25	16	16	0.5	0.12
2bd	b	d	0.5	8	4	0.5	0.03
2be	b	e	0.25	4	4	0.06	0.03
2cd	c	d	0.015	0.5	0.25	0.06	0.06
2ce	c	e	0.03	1	2	0.06	0.06
2cf	c	f	0.015	1	1	0.002	N.D.
2cg	c	g	0.12	0.25	0.5	0.06	0.03
2ch	c	h	0.5	1	4	0.25	0.25
2dd	d	d	0.12	4	4	0.06	0.03
2de	d	e	0.5	8	8	0.03	0.015
2df	d	f	0.25	8	4	0.12	0.015
2di	d	i	1	8	32	0.06	N.D.

[a]Ef (*E. faecalis* ATCC 29212), Sa (*S. aureus* ATCC 29213), Ec (*E. coli* ATCC 25922), Ms (*M. smegmatis* ATCC 19420), Mt (*M. tuberculosis* H37Rv). N.D. (not determined).

Table 1. *In vitro* antibacterial activity of novobiocin **1** and amide-linked pyrimido[4,5-*b*]indol-8-amine inhibitors.

Compound	MIC (μg/mL)[a] Ab	Pa	Hi	Se	Sp	HepG2 (IC_{50}, μg/mL)[b]
Novobiocin **1**	N.D.	>64 (ref.[15])	0.5 (ref.[15])	0.06 (ref.[15])	0.5 (ref.[15])	>32
2ac	16	128	1	1	0.12	10.82
2ad	8	32	1	1	1	>16
2bd	>64	>64	4	2	2	>32
2cd	1	>64	4	0.12	0.12	>16

[a]Ab (*A. baumannii* NCTC 13420), Pa (*P. aeruginosa* ATCC 27853), Hi (*H. influenzae* ATCC 49247), Se (*S. epidermidis* ATCC 12228), Sp (*S. pneumoniae* ATCC 49619) [b]Hep G2 cells incubated for 24 h at 37 °C in 5% CO_2 and viability determined using CellTiter-Glo® (Promega, WI, USA). N.D. (not determined).

Table 2. Extended *in vitro* antibacterial activity and cytotoxicity of novobiocin **1** and a selected amide-linked pyrimido[4,5-*b*]indol-8-amine inhibitors.

Compound	*M. tuberculosis* gyrase supercoiling inhibition (IC_{50}, μM)	*M. tuberculosis* gyrase ATPase inhibition (IC_{50}, μM)	Human topoisomerase II decatenation inhibition (% inhibition at 100 μM)
Novobiocin **1**	0.085	0.020	N.D.
2ac	0.005	0.025	5.8%
2ad	0.010	0.059	21.2%

Table 3. Target engagement of novobiocin **1** and selected amide-linked pyrimido[4,5-*b*]indol-8-amine inhibitors. N.D. (not determined).

Compound	MIC (μg/mL)[a]				
	Ms	Mt	FQ-R1 (GyrA D94N substitution)	INH-R1 (truncated at 155 of KatG)	RIF-R1 (RpoB S522L substitution)
Moxifloxacin (FQ)	0.03	N.D.	3.9	0.04	0.04
Isoniazid (INH)	4	N.D.	0.05	>27	0.014
Rifampicin (RIF)	16	N.D.	0.019	0.013	3.0
Novobiocin **1**	1	4 (ref.[16])	7.35	6.7	13.5
2ac	0.12	N.D.	0.014	0.013	0.012
2ad	0.25	0.25	0.09	0.09	0.09

[a]Ms (*M. smegmatis* ATCC 19420), Mt (*M. tuberculosis* H37Rv), FQ-R1 (fluoroquinolone-resistant), INH-R1 (isoniazid-resistant), RIF-R1 (rifampicin-resistant). N.D. (not determined). Data collected in May 2015.

Table 4. *In vitro* antibacterial activity of clinically used antibiotics and amide-linked pyrimido[4,5-*b*]indol-8-amine inhibitors against resistant isolates.

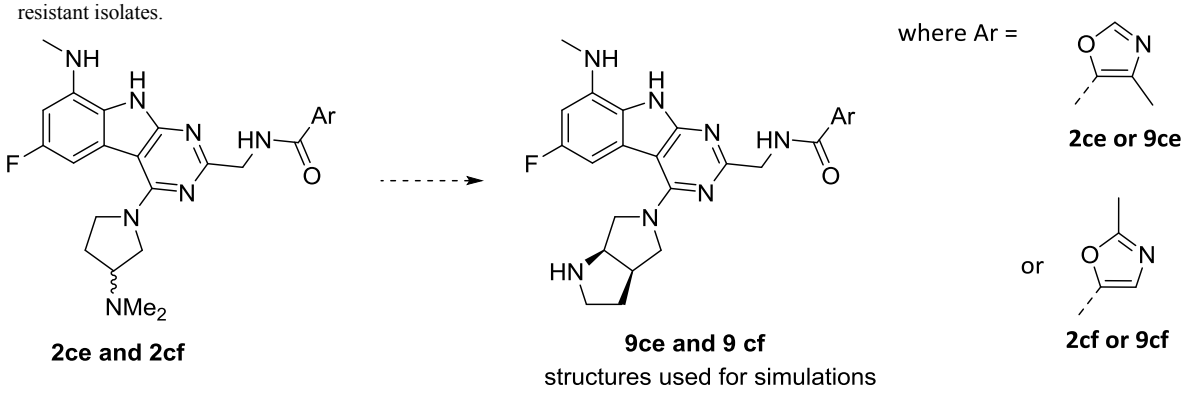

Figure 3. **9ce**, and **9cf** were used for the computational analysis, as analogues of **2ce** and **2cf** respectively.

COMPUTATIONAL ANALYSIS

Compound **2cf**, the result of 2-methylation of the oxazole in **2cd**, was found to be 5-fold higher in potency against *M. smegmatis* compared to the undecorated analogue. Although it was hypothesised that the addition of the methyl group may result in improved permeability through increasing lipophilicity, computational simulations were used to determine if the potency increase was due to a specific interaction. Molecular dynamics calculations were performed using Desmond v2.3[17] (see **Experimental** section, below) on two hypothetical analogues relating to **2ce** and **2cf** (**9ce** and **9cf, Figure 3**). As the most structurally similar analogue with an X-ray crystal structure (PDB: 4K4O[10]) utilised a bicyclic amine in the amine pocket, this was kept consistent throughout the simulations to ensure differences in binding could be rationalised primarily through alterations to the heterocycle inhabiting the side-chain pocket.

The simulation showed that the protein-ligand interactions were stable, and key interactions were consistent with those observed in the X-ray crystal structure of similar GyrB inhibitors, providing confidence in the computational method. The most important binding interactions were found to be hydrogen bonds between the three nitrogen atoms on the tricyclic core and Asp73 and its coordinated water. Furthermore, a strong association of the oxazole ring with Arg76 was concordant with a π-cation interaction, consistent with published observations.[10] As the core of the molecule remained unchanged throughout the simulations, focus was placed on how the heterocyclic amide may effect binding. The resulting interaction maps for the oxazole substituents are shown in **Figure 4**, with relative interaction probabilities annotated alongside. For example, an interaction probability of 61% related to the interaction being observed to occur during 61% of the simulation.

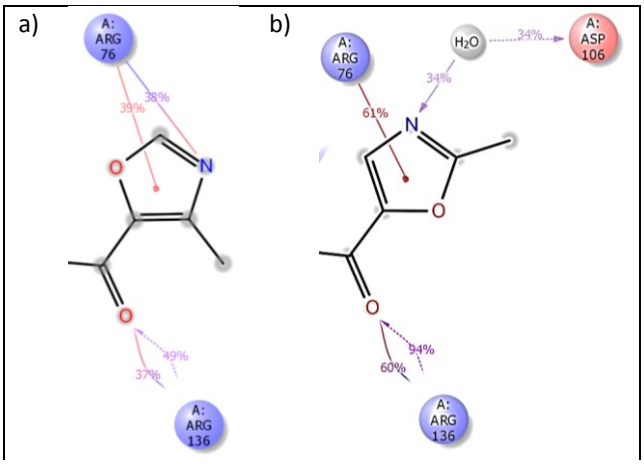

Figure 4. Interaction maps for structures relating to a) **9ce** and b) **9cf**

Similar residues were observed to be involved in each compound's binding interactions near the amide substituent, however, the extent of the binding was variable. Arg136 formed a hydrogen bond with the amide carbonyl in both simulations. However, in **9cf**, this interaction seemed more stable, with a higher interaction probability (up to 94% compared to up to 49% in **9ce**). This improved interaction in **9cf** was hypothesised to be a result of the oxazole-methyl group in **9cf** causing a steric clash with Arg136 in the active site, discouraging binding (**Figure 5a**). Movement of the methyl group to the 2-position of the oxazole could alleviate this clash, decreasing the overall energy of the system, and contributing to an increase the potency of the ligand.

a)

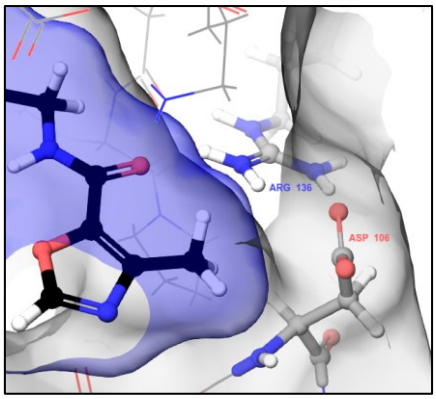

b)

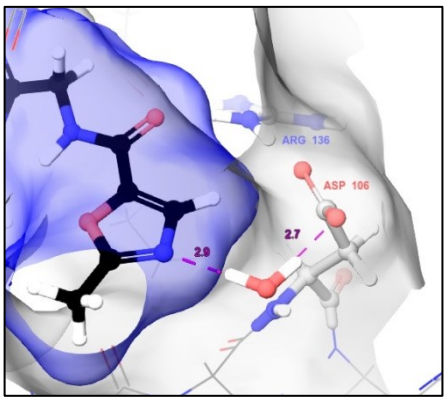

Figure 5. a) Potential clash of Arg136 with **9ce**, which would be alleviated in **9cf** b) MD frame of **9cf** highlighting the possible water-mediated interaction made with Asp106.

Interestingly, an additional potency driving interaction may be picked up by **9cf** to Asp106, which resides on the flexible loop commonly omitted from the majority of deposited X-ray crystal structures. The nitrogen atom in the oxazole ring of **9cf** may be in a more appropriate orientation to bind *via* a water-mediated interaction to Asp106 (**Figure 5b**). The existence of this interaction may reflect the increase in *M. smegmatis* potency observed between compounds **2ce** and **2cf**. Furthermore, elaboration along the vector towards Asp106 may provide additional potency-driving interactions to optimise the series.

In summary, utilising computational analysis of previously published crystal structures of GyrB inhibitors in DNA gyrase allowed the development of the current antibacterial series, focussing on improving the activity and spectrum of susceptible bacteria. A combination of expanding into an identified area of the active site, and alteration of permeability through removal of H-bond donors, has successfully yielded antibacterial compounds with potent activity against gram-positive bacteria and mycobacteria. Furthermore, the potential of the series has been exemplified through the ability of the compounds to maintain activity against a range of drug-resistant *M. tuberculosis* clinical isolates. Subsequent alterations of the amide-linked heterocycles have demonstrated steric bulk can not only be tolerated in this area of the protein, but additional potency increasing interactions could be designed into the inhibitors through interaction with Asp106, which resides on the flexible loop.

EXPERIMENTAL

Molecular dynamics

Protein structures were prepared using Maestro's Protein Preparation Wizard (PrepWizard), following the procedure outlined by Sastry *et al.*[18] Unfortunately, the X-ray crystal structure of 4K4O[10] (*E. faecalis*) was not complete, and the flexible loop of residues that resided near the pyrimidine substituent were omitted, resulting in the use of a complete crystal structure, 3G7E[12] (*E. coli*), instead. The suitability of the proteins to be interchanged was assessed by determining that 68% of residues within the active site were identical. Of the non-identical residues, mutation was commonly observed to be a result of a small change (e.g VAL to ILE). Each mutated residue was assessed for its contribution to binding, resulting in 95% similarity of the active sites of 4K4O and 3G7E, and could therefore used interchangeably during the computational studies. Furthermore, both sequences were seen to be highly similar to 3ZM7 (*M. tuberculosis*), allowing comparisons in binding to be drawn from simulations of 3G7E. Each compound was docked using a knowledge-based alignment and the protein-ligand complex was solvated and simulated for 8 ns at a temperature of 300K using the OPLS_2005 force field[19] in Desmond v2.3.[17] The system trajectories were then analysed using Maestro v10.6.014[14], monitoring how key interactions evolved over the course of the experiment.

DECLARATION OF INTEREST

All authors affiliated with Redx Pharma are/were employees of the company and may own shares and/or share options in Redx Pharma Plc.

FUNDING

This research did not receive any specific grant from funding agencies in the public, commercial, or not-for-profit sectors. DNA topology and gyrase ATPase assays were performed by Inspiralis Ltd (Norwich, United Kingdom). This work was supported in part by National Institutes of Health and the National Institute of Allergy and Infectious Diseases, Contract No. HHSN272201100009I.

REFERENCES

1. O'Neill J. Tackling Drug-Resistant Infections Globally: Final Report and Recommendations. **2016**.
2. *Fact Sheet 104: Tuberculosis*. World Health Organisation; October **2017**.
3. Allen HK, Donato J, Wang HH, Cloud-Hansen KA, Davies J, Handelsman J. Call of the wild: antibiotic resistance genes in natural environments. *Nat. Rev. Micro.* **2010**;8(4): 251-259.
4. Vos SM, Tretter EM, Schmidt BH, Berger JM. All tangled up: how cells direct, manage and exploit topoisomerase function. *Nat. Rev. Mol. Cell Biol.* **2011**;12(12): 827-841.

5. Charifson PS, Grillot A-L, Grossman TH, *et al*. Novel Dual-Targeting Benzimidazole Urea Inhibitors of DNA Gyrase and Topoisomerase IV Possessing Potent Antibacterial Activity: Intelligent Design and Evolution through the Judicious Use of Structure-Guided Design and Stucture−Activity Relationships. *J. Med. Chem.* **2008**;51(17): 5243-5263.
6. Starr JT, Sciotti RJ, Hanna DL, *et al*. 5-(2-Pyrimidinyl)-imidazo[1,2-a]pyridines are antibacterial agents targeting the ATPase domains of DNA gyrase and topoisomerase IV. *Bioorg. Med. Chem. Lett.* **2009**;19(18): 5302-5306.
7. Grillot A-L, Tiran AL, Shannon D, *et al*. Second-Generation Antibacterial Benzimidazole Ureas: Discovery of a Preclinical Candidate with Reduced Metabolic Liability. *J. Med. Chem.* **2014**;57(21): 8792-8816.
8. Manchester JI, Dussault DD, Rose JA, *et al*. Discovery of a novel azaindole class of antibacterial agents targeting the ATPase domains of DNA gyrase and Topoisomerase IV. *Bioorg. Med. Chem. Lett.* **2012**;22(15): 5150-5156.
9. East SP, White CB, Barker O, *et al*. DNA gyrase (GyrB)/topoisomerase IV (ParE) inhibitors: Synthesis and antibacterial activity. *Bioorg. Med. Chem. Lett.* **2009**;19(3): 894-899.
10. Tari LW, Li X, Trzoss M, *et al*. Tricyclic GyrB/ParE (TriBE) Inhibitors: A New Class of Broad-Spectrum Dual-Targeting Antibacterial Agents. *PLOS ONE.* **2013**;8(12): e84409.
11. Cooper I, Pichowicz M, Stokes N. WO 2016067009. **2016**.
12. Ronkin SM, Badia M, Bellon S, *et al*. Discovery of pyrazolthiazoles as novel and potent inhibitors of bacterial gyrase. *Bioorg. Med. Chem. Lett.* **2010**;20(9): 2828-2831.
13. Zhang J, Yang Q, Cross JB, *et al*. Discovery of Azaindole Ureas as a Novel Class of Bacterial Gyrase B Inhibitors. *J. Med. Chem.* **2015**;58(21): 8503-8512.
14. Schrödinger Release 2017-3 : Maestro, Schrödinger, LLC, New York, NY, **2017**.
15. Stokes NR, Thomaides-Brears HB, Barker S, *et al*. Biological evaluation of benzothiazole ethyl urea inhibitors of bacterial type II topoisomerases. *Antimicrob Agents Chemother.* **2013**;57(12): 5977-5986.
16. Chopra S, Matsuyama K, Tran T, *et al*. *J Antimicrob Chemother.* **2012**;67(2): 415-421.
17. Bowers KJ, Chow E, Xu H, *et al*. Scalable algorithms for molecular dynamics simulations on commodity clusters. *Proceedings of the 2006 ACM/IEEE conference on Supercomputing*. Tampa, Florida: ACM; **2006**:84.
18. Sastry MG, Adzhigirey M, Day T, Annabhimoju R, Sherman W. Protein and ligand preparation: parameters, protocols, and influence on virtual screening enrichments. *J. Comput. Aided. Mol. Des.* **2013**;27(3): 221-234.
19. Shivakumar D, Williams J, Wu Y, Damm W, Shelley J, Sherman W. Prediction of Absolute Solvation Free Energies using Molecular Dynamics Free Energy Perturbation and the OPLS Force Field. *J. Chem. Theory Comput.* **2010**;6(5): 1509-1519.

Design, synthesis and antibacterial properties of pyrimido[4,5-*b*]indol-8-amine inhibitors of DNA gyrase

David H. McGarry[a,*], Ian R. Cooper[a], Rolf Walker[a], Catherine E. Warrilow[a], Mark Pichowicz[a], Andrew J. Ratcliffe[a], Anne-Marie Salisbury[a], Victoria J. Savage[a], Emmanuel Moyo[a], John Maclean[a], Andrew Smith[a], Cédric Charrier[a], Neil R. Stokes[a], David M. Lindsay[b], William J. Kerr[b].

[a]Redx Pharma, Alderley Park, Cheshire, SK10 4TG, United Kingdom [b]Department of Pure and Applied Chemistry, University of Strathclyde, WestCHEM, Thomas Graham Building, 295 Cathedral Street, Glasgow, G1 1XL,United Kingdom

Supporting information

General remarks

NMR spectra were obtained on a LC Bruker AV500 using a 5 mm QNP probe. Coupling constants are reported in Hz and refer to $^3J_{H\text{-}H}$ interactions unless otherwise stated.

LCMS was carried out on a Waters Alliance ZQ MS using H_2O and MeCN mobile phase with pH modification as detailed below. Wavelengths measured were 254 and 210 nm.

LCMS Method (Basic pH)

Column: YMC-Triart C_{18} 50 × 2 mm, 5 µm. Flow rate: 0.8 mL/min. Injection volume: 5 µL.

Mobile Phase
A H_2O
B MeCN
C 50% H_2O / 50% MeCN + 1.0% ammonia

Time (min)	A (%)	B (%)	C (%)
0	95	0	5
4	0	95	5
4.4	0	95	5
4.5	95	5	0
4.5	STOP		

Table 1

Pyrrolidines							
a	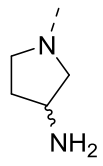	**b**	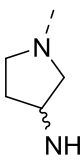	**c**	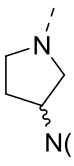	**d**	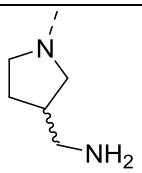
Amides							
a	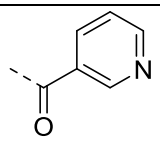	**b**	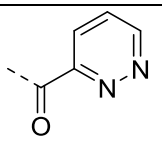	**c**	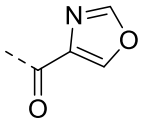		
d	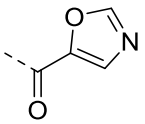	**e**	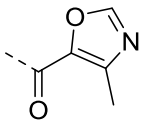	**f**	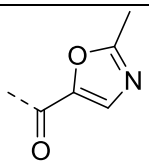		
g	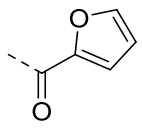	**h**	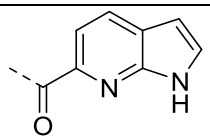	**i**	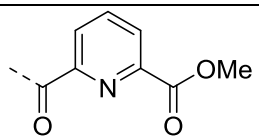		
Compounds contained within the Supplementary Information section are, where appropriate, numbered by pyrrolidine then amide. i.e. where pyrrolidine **a** and amide **b** are used, the final compound title is **2ab**.							

Table 2

Procedures

General procedure for the synthesis of pyrrolidine substituted intermediates (4a-d)

Following the general procedure below, the data are reported as a) mass of starting material; b) mass of pyrrolidine; c) mass of K_2CO_3; d) volume of ethanol; e) mass of product obtained.

Following an adapted procedure of Bensen *et al*.,[63] to a microwave vial was added *tert*-butyl *N*-[2,4-bis(benzylsulfonyl)-6-fluoro-9*H*-pyrimido[4,5-*b*]indol-8-yl]-*N*-methyl-carbamate **3** (1.12 - 4.80 mmol, 1 eq), corresponding pyrrolidine (either a) *tert*-butyl pyrrolidin-3-ylcarbamate, b) *tert*-butyl methyl(pyrrolidin-3-yl)carbamate, c) *N*,*N*-dimethylpyrrolidin-3-amine or d) *tert*-butyl (pyrrolidin-3-ylmethyl)carbamate) (1.46 - 5.28 mmol, 1.3 eq) and potassium carbonate (1.74 - 5.76 mmol, 1.5 eq) in EtOH. The mixture was heated in a Biotage Initiator microwave reactor at 45 °C for 50 min. The mixture was concentrated *in vacuo* and the resulting solid was dissolved in EtOAc, then washed with water then brine. The organic phase was concentrated *in vacuo* and purified by silica gel column chromatography (gradient = 0-100% EtOAc in petroleum ether (bp. 40-60)). The appropriate fractions were combined and concentrated *in vacuo* to give pyrrolidine-substituted intermediates **4a-d** in good yield.

***tert*-butyl *N*-[2-benzylsulfonyl-4-[3-(*tert*-butoxycarbonylamino)pyrrolidin-1-yl]-6-fluoro-9*H*-pyrimido[4,5-*b*]indol-8-yl]-*N*-methyl-carbamate (4a)**

Following the general procedure above: a) 3 g; b) 3-Boc-aminopyrrolidine, 984 mg; c) 996 mg; d) 30 mL; e) 1.87 g.

Yellow solid; yield 75%; LCMS: R_T = 3.14 min, [M+H]+ 655.5; ^{1}H NMR (400 MHz, $CDCl_3$) δ_H 9.21 (s, 1H), 7.62 (dd, $^3J_{H\text{-}F}$ = 9.8 Hz, $^4J_{H\text{-}H}$ = 2.3 Hz, 1H), 7.42 – 7.33 (m, 2H), 7.33 – 7.25 (m, 3H), 7.05 (dd, $^3J_{H\text{-}F}$ = 9.8 Hz, $^4J_{H\text{-}H}$ = 2.3 Hz, 1H), 4.79 – 4.72 (m, 3H), 4.47 – 4.32 (m, 1H), 4.23 – 4.21 (m, 1H), 4.08 – 3.95 (m, 2H), 3.84 (m, 1H), 3.34 (s, 3H), 2.37 – 2.24 (m, 1H), 2.12 – 2.05 (m, 1H), 1.49 (s, 18H).

***tert*-butyl *N*-[1-[2-benzylsulfonyl-8-[*tert*-butoxycarbonyl(methyl)amino]-6-fluoro-9*H*-pyrimido[4,5-*b*]indol-4-yl]pyrrolidin-3-yl]-*N*-methyl-carbamate (4b)**

Following the general procedure above: a) 1.02 g; b) -(*N*-Boc-*N*-methylamino)pyrrolidine, 0.40 mL; c) 344 mg; d) 5 mL; e) 700 mg.

Off-white solid; yield 64%; LCMS: R_T = 3.78 min, [M+H]+ 669.5; ^{1}H NMR (500 MHz, $CDCl_3$) δ_H 9.30 (s, 1H), 7.61 (dd, $^3J_{H\text{-}F}$ = 9.8 Hz, $^4J_{H\text{-}H}$ = 2.3 Hz, 1H), 7.41 – 7.35 (m, 2H), 7.31 – 7.26 (m, 3H), 7.06 (dd, $^3J_{H\text{-}F}$ = 9.8 Hz, $^4J_{H\text{-}H}$ = 2.3 Hz, 1H), 4.91 – 4.69 (m, 3H), 4.12 – 3.99 (m, 3H), 3.93 – 3.84 (m, 1H), 3.33 (s, 3H), 2.88 (s, 3H), 2.29 – 2.10 (m, 2H), 1.49 (s, 18H).

***tert*-butyl *N*-[2-benzylsulfonyl-4-[3-(dimethylamino)pyrrolidin-1-yl]-6-fluoro-9*H*-pyrimido[4,5-*b*]indol-8-yl]-*N*-methyl-carbamate (4c)**

Following the general procedure above: a) 700 mg; b) *N*,*N*-dimethylpyrrolidin-3-amine, 0.16 mL; c) 241 mg; d) 5 mL; e) 580 mg.

Off-white solid; yield 89%; LCMS: R_T = 3.34 min, [M+H]+ 583.2; ^{1}H NMR (500 MHz, $CDCl_3$) δ_H 9.02 (s, 1H), 7.65 (dd, $^3J_{H\text{-}F}$ = 9.8 Hz, $^4J_{H\text{-}H}$ = 2.2 Hz, 1H), 7.42 – 7.36 (m, 2H), 7.32 – 7.28 (m, 3H), 7.04 (dd, $^3J_{H\text{-}F}$ = 9.8 Hz, $^4J_{H\text{-}H}$ = 2.2 Hz, 1H), 4.81 – 4.70 (m, 2H), 4.18 – 4.00 (m, 3H), 3.89 (dd, *J* = 10.3, 8.3 Hz, 1H), 3.34 (s, 3H), 2.84 (p, *J* = 7.2, 6.6 Hz, 1H), 2.36 (s, 6H), 2.27 (s, 1H), 2.04 – 1.97 (m, 1H), 1.47 (s, 9H).

tert-butyl _N_-[2-benzylsulfonyl-4-[3-[(_tert_-butoxycarbonylamino)methyl]pyrrolidin-1-yl]-6-fluoro-9_H_-pyrimido[4,5-_b_]indol-8-yl]-_N_-methyl-carbamate (4d)

Following the general procedure above: a) 1.2 g; b) *tert*-butyl-(pyrrolidin-3-ylmethyl)carbamate, 0.42 mL; c) 392 mg; d) 4 mL; e) 780 mg.

Off-white solid; yield 61%; LCMS: R_T = 3.66 min, [M+H]+ 669.2; ^{1}H NMR (500 MHz, $CDCl_3$) δ_H 9.54 (s, 1H), 7.68 (d, $^3J_{H-F}$ = 9.8 Hz, 1H), 7.37 (s, 2H), 7.31 – 7.27 (m, 3H), 7.04 (d, $^3J_{H-F}$ = 9.8 Hz, 1H), 4.81 – 4.69 (m, 2H), 4.10 – 3.98 (m, 3H), 3.78 – 3.72 (m, 1H), 3.33 (s, 3H), 3.31 – 3.20 (m, 2H), 2.57 – 2.53 (m, 1H), 2.22 – 2.14 (m, 1H), 1.88 – 1.78 (m, 1H), 1.45 (s, 18H).

General procedure for the synthesis of nitrile substituted intermediates (5a-d)

Following the general procedure below, the data are reported as a) mass of starting material; b) mass of sodium cyanide; c) volume of DMF; d) mass of product obtained.

A solution of sulfone intermediate **4a-d** (1.00 – 2.86 mmol, 1 eq) and sodium cyanide (2.10 – 3.14 mmol, 1.1-2.1 eq) in DMF was heated to 100 °C for 16 h. The reaction mixture was poured into water and extracted with EtOAc. The combined organics were extracted with water, brine, dried ($MgSO_4$), filtered and concentrated *in vacuo* to give the crude product which was purified by silica gel column chromatography (gradient = 0-100% EtOAc in petroleum ether (bp. 40-60)). The appropriate fractions were combined and concentrated *in vacuo* to give the corresponding nitrile substituted intermediates **5a-d** in good to excellent yield.

tert-butyl *N*-[4-[3-(*tert*-butoxycarbonylamino)pyrrolidin-1-yl]-2-cyano-6-fluoro-9*H*-pyrimido[4,5-*b*]indol-8-yl]-*N*-methyl-carbamate (5a)

Following the general procedure above: a) *tert*-butyl *N*-[2-benzylsulfonyl-4-[3-(*tert*-butoxycarbonylamino)pyrrolidin-1-yl]-6-fluoro-9*H*-pyrimido[4,5-*b*]indol-8-yl]-*N*-methyl-carbamate 1.87 g; b) 150 mg; c) 27 mL; d) 1.29 g.

White solid; yield 86%; LCMS: R_T = 3.21 min, [M+H]+ 526.5; ^{1}H NMR (400 MHz, $CDCl_3$) δ 9.11 (s, 1H), 7.61 (dd, $^3J_{H\text{-}F}$ = 9.8 Hz, $^4J_{H\text{-}H}$ = 2.3 Hz, 1H), 7.05 (dd, $^3J_{H\text{-}F}$ = 9.8 Hz, $^4J_{H\text{-}H}$ = 2.3 Hz, 1H), 4.88 – 4.59 (m, 1H), 4.40 – 4.37 (m, 1H), 4.25 – 4.17 (m, 1H), 4.10 – 3.96 (m, 2H), 3.87 – 3.78 (m, 1H), 3.35 (s, 3H), 2.38 – 2.25 (m, 1H), 2.13 – 2.00 (m, 1H), 1.46 (s, 18H).

tert-butyl *N*-[1-[8-[*tert*-butoxycarbonyl(methyl)amino]-2-cyano-6-fluoro-9*H*-pyrimido[4,5-*b*]indol-4-yl]pyrrolidin-3-yl]-*N*-methyl-carbamate (5b)

Following the general procedure above: a) *tert*-butyl *N*-[1-[2-benzylsulfonyl-8-[*tert*-butoxycarbonyl(methyl)amino]-6-fluoro-9*H*pyrimido[4,5-*b*]indol-4-yl]pyrrolidin-3-yl]-*N*-methyl-carbamate 790 mg; b) 122 mg; c) 13 mL; d) 380 mg.

Yellow solid; yield 60%; LCMS: R_T = 3.84 min, [M+H]+ 540.6; ^{1}H NMR (500 MHz, $CDCl_3$) δ_H 9.35 (s, 1H), 7.60 (dd, $^3J_{H\text{-}F}$ = 9.8 Hz, $^4J_{H\text{-}H}$ = 2.3 Hz, 1H), 7.06 (dd, $^3J_{H\text{-}F}$ = 9.8 Hz, $^4J_{H\text{-}H}$ = 2.3 Hz, 1H), 4.91 – 4.83 (s, 1H), 4.09 – 3.95 (m, 3H), 3.92 – 3.84 (m, 1H), 3.35 (s, 3H), 2.89 (s, 3H), 2.29 – 2.11 (m, 2H), 1.49 (s, 18H).

tert-butyl *N*-[2-cyano-4-[3-(dimethylamino)pyrrolidin-1-yl]-6-fluoro-9*H*-pyrimido[4,5-*b*]indol-8-yl]-*N*-methyl-carbamate (5c)

Following the general procedure above: a) *tert*-butyl *N*-[2-benzylsulfonyl-4-[3-(dimethylamino)pyrrolidin-1-yl]-6-fluoro-9*H*pyrimido[4,5-*b*]indol-8-yl]-*N*-methyl-carbamate 580 mg; b) 103 mg; c) 11 mL; d) 310 mg.

Brown solid; yield 69%; LCMS: R_T = 3.35 min, [M+H]+ 454.2; ^{1}H NMR (500 MHz, $CDCl_3$) δ_H 9.35 (s, 1H), 7.64 (dd, $^3J_{H\text{-}F}$ = 9.9 Hz, $^4J_{H\text{-}H}$ = 2.2 Hz, 1H), 7.04 (dd, $^3J_{H\text{-}F}$ = 9.7 Hz, $^4J_{H\text{-}H}$ = 2.2 Hz, 1H), 4.14 – 3.97 (m, 3H), 3.86 (dd, *J* = 10.4, 8.2 Hz, 1H), 3.35 (s, 3H), 2.87 – 2.78 (m, 1H), 2.37 (s, 6H), 2.29 – 2.25 (m, 1H), 2.03 – 1.96 (m, 1H), 1.46 (s, 9H).

tert-butyl _N_-[4-[3-[(_tert_-butoxycarbonylamino)methyl]pyrrolidin-1-yl]-2-cyano-6-fluoro-9_H_-pyrimido[4,5-_b_]indol-8-yl]-_N_-methyl-carbamate (5d)

Following the general procedure above: a) *tert*-butyl *N*-[2-benzylsulfonyl-4-[3-[(*tert*-butoxycarbonylamino)methyl]pyrrolidin-1-yl]-6-fluoro-9*H*-pyrimido[4,5-*b*]indol-8-yl]-*N*-methyl-carbamate 780 mg; b) 114 mg; c) 15 mL; d) 560 mg.

Yellow solid; yield 89%; LCMS: R_T = 3.72 min, [M+H]+ 540.2, 484.1; ^{1}H NMR (500 MHz, $CDCl_3$) δ_H 9.08 (s, 1H), 7.68 (d, $^3J_{H\text{-}F}$ = 9.8 Hz, 1H), 7.04 (dd, $^3J_{H\text{-}F}$ = 9.8 Hz, $^4J_{H\text{-}H}$ = 2.3 Hz, 1H), 4.83 – 4.73 (m, 1H), 4.10 – 3.95 (m, 3H), 3.75 – 3.72 (m, 1H), 3.35 (s, 3H), 3.34 – 3.20 (m, 2H), 2.59 – 2.53 (m, 1H), 2.21 – 2.17 (m, 1H), 1.84 – 1.80 (m, 1H), 1.46 (s, 18H).

General procedure for the reduction of nitrile substituted intermediates (6a-d)

Following the general procedure below, the data are reported as a) mass of starting material; b) volume of Raney nickel used; c) volume of ethanol; d) mass of product obtained.

To a solution of corresponding nitrile intermediate **5a-d** (0.10 – 1.04 mmol) in EtOH was added Raney nickel (aq. slurry). The flask was evacuated and purged with hydrogen 3 times then stirred at RT for 16 h under an atmosphere of hydrogen. The reaction mixture was filtered through celite, extracted with MeOH and concentrated *in vacuo* to furnish the corresponding amine product **6a-d** in good yield.

***tert*-butyl *N*-[1-[2-(aminomethyl)-8-[*tert*-butoxycarbonyl(methyl)amino]-6-fluoro-9*H*-pyrimido[4,5-*b*]indol-4-yl]pyrrolidin-3-yl]-*N*-methyl-carbamate (6a)**

Following the general procedure above: a) *tert*-butyl *N*-[4-[3-(*tert*-butoxycarbonylamino)pyrrolidin-1-yl]-2-cyano-6-fluoro-9*H*-pyrimido[4,5-*b*]indol-8-yl]-*N*-methyl-carbamate 500 mg; b) 2 mL; c) 15 mL; d) 446 mg.

Orange solid; yield 89%; LCMS: R_T = 1.90 min, [M+H]+ 530.5.

***tert*-butyl *N*-[1-[2-(aminomethyl)-8-[*tert*-butoxycarbonyl(methyl)amino]-6-fluoro-9*H*-pyrimido[4,5-*b*]indol-4-yl]pyrrolidin-3-yl]-*N*-methyl-carbamate (6b)**

Following the general procedure above: a) *tert*-butyl *N*-(4-benzylsulfonyl-2-cyano-6-fluoro-9*H*-pyrimido[4,5-*b*]indol-8-yl)-*N*-methyl-carbamate 350 mg; b) 1 mL; c) 15 mL; d) 342 mg.

Brown solid; yield 97%; LCMS: R_T = 4.01 min, [M+H]+ 544.6.

***tert*-butyl *N*-[2-(aminomethyl)-4-[3-(dimethylamino)pyrrolidin-1-yl]-6-fluoro-9*H*-pyrimido[4,5-*b*]indol-8-yl]-*N*-methyl-carbamate (6c)**

Following the general procedure above: a) *tert*-butyl *N*-[2-(aminomethyl)-4-[3-(dimethylamino)pyrrolidin-1-yl]-6-fluoro-9*H*-pyrimido[4,5-*b*]indol-8-yl]-*N*-methyl-carbamate 310 mg; b) 2 mL; c) 15 mL; d) 214 mg.

Orange solid; yield 68%; LCMS: R_T = 2.58 min, [M+H]+ 458.2.

***tert*-butyl *N*-[2-(aminomethyl)-4-[3-[(*tert*-butoxycarbonylamino)methyl]pyrrolidin-1-yl]-6-fluoro-9*H*-pyrimido[4,5-*b*]indol-8-yl]-*N*-methyl-carbamate (6d)**

Following the general procedure above: a) *tert*-butyl *N*-[4-[3-[(*tert*-butoxycarbonylamino)methyl]pyrrolidin-1-yl]-2-cyano-6-fluoro-9*H*-pyrimido[4,5-*b*]indol-8-yl]-*N*-methyl-carbamate 560 mg; b) 2 mL; c) 15 mL; d) 423 mg.

Orange solid; yield 75%; LCMS: R_T = 3.09 min, [M+H]+ 544.3.

General procedure synthesis of Boc-protected final compounds (7)

Following the general procedure below, the data are reported as a) mass of starting material; b) mass of acid; c) mass of EDCI; d) volume of DCM; e) volume of NEt_3; f) mass of product obtained.

To an ice cold solution of corresponding primary amine **6a-d** (0.05 - 0.38 mmol, 1 eq), corresponding acid (0.06 - 0.48 mmol, 1.3 eq) and EDCI (0.05 - 0.49 mmol, 1.3 eq) in DCM was added NEt_3 (0.06 - 0.53 mmol, 1.4 eq) and the mixture was warmed to RT and stirred for 16 h. The reaction mixture was loaded directly onto a pre-equilibrated silica column and purified by silica gel column chromatography (gradient = 0-100% EtOAc in petroleum ether (bp. 40-60)). The appropriate fractions were combined and concentrated *in vacuo* to give the corresponding Boc-protected final compound **7**.

tert-butyl _N_-[4-[3-(_tert_-butoxycarbonylamino)pyrrolidin-1-yl]-6-fluoro-2-[(pyridine-3-carbonylamino)methyl]-9_H_-pyrimido[4,5-_b_]indol-8-yl]-_N_-methyl-carbamate (7aa)

Following the general procedure above: a) *tert*-butyl *N*-[2-(aminomethyl)-4-[3-(*tert*-butoxycarbonylamino)pyrrolidin-1-yl]-6-fluoro-9*H*-pyrimido[4,5-*b*]indol-8-yl]-*N*-methyl-carbamate 30 mg; b) Nicotinic acid 8 mg; c) 11 mg; d) 2 mL; e) 10 µL; f) 7 mg.

Yellow oil; yield 18%; LCMS: R_T = 3.08 min, [M+H]+ 625.3; ^{1}H NMR (400 MHz, CD_3OD) δ_H 9.03 (s, 1H), 8.63 (s, 1H), 8.25 (s, 1H), 7.67 (s, 1H), 7.62 (dd, $^3J_{H\text{-}F}$ = 10.4 Hz, $^4J_{H\text{-}H}$ = 2.3 Hz, 1H), 6.93 (dd, $^3J_{H\text{-}F}$ = 10.4 Hz, $^4J_{H\text{-}H}$ = 2.3 Hz, 1H), 4.52 (s, 2H), 4.18 – 3.93 (m, 3H), 3.92 – 3.81 (m, 1H), 3.74 – 3.67 (m, 1H), 3.22 – 3.17 (m, 6H), 2.21 – 2.07 (m, 1H), 2.00 – 1.83 (m, 1H), 1.33 (s, 18H).

tert-butyl _N_-[4-[3-(_tert_-butoxycarbonylamino)pyrrolidin-1-yl]-6-fluoro-2-[(pyridazine-3-carbonylamino)methyl]-9_H_-pyrimido[4,5-_b_]indol-8-yl]-_N_-methyl-carbamate (7ab)

Following the general procedure above: a) *tert*-butyl 2-[1-[2-(aminomethyl)-8-[*tert*-butoxycarbonyl(methyl)amino]-6-fluoro-9*H*-pyrimido[4,5-*b*]indol-4-yl]pyrrolidin-3-yl]acetate 30 mg; b) pyridazine-3-carboxylic acid 7 mg; c) 9 mg; d) 2 mL; e) 8 µL; f) 4 mg.

Yellow oil; yield 13%; LCMS: R_T = 2.71 min, [M+H]+ 636.6.

tert-butyl _N_-[4-[3-(tert-butoxycarbonylamino)pyrrolidin-1-yl]-6-fluoro-2-[(oxazole-4-carbonylamino)methyl]-9_H_-pyrimido[4,5-_b_]indol-8-yl]-_N_-methyl-carbamate (7ac)

Following the general procedure above: a) *tert*-butyl *N*-[2-(aminomethyl)-4-[3-(*tert*-butoxycarbonylamino)pyrrolidin-1-yl]-6-fluoro-9*H*-pyrimido[4,5-*b*]indol-8-yl]-*N*-methyl-carbamate 50 mg; b) oxazole-4-carboxylic acid 21 mg; c) 29 mg; d) 10 mL; e) 40 µL; f) 22 mg.

Yellow oil; yield 45%; LCMS R_T = 2.76 min, [M+H]+ 625.6; ^{1}H NMR (400 MHz, CD_3OD) δ_H 8.33 (d, $^4J_{H\text{-}H}$ = 1.0 Hz, 1H), 8.14 (d, $^4J_{H\text{-}H}$ = 1.0 Hz, 1H), 7.63 (dd, $^3J_{H\text{-}F}$ = 10.4 Hz, $^4J_{H\text{-}H}$ = 2.3 Hz, 1H), 6.94 (dd, $^3J_{H\text{-}F}$ = 10.4 Hz, $^4J_{H\text{-}H}$ = 2.3 Hz, 1H), 4.52 (s, 2H), 4.15 – 3.96 (m, 3H), 3.91 – 3.87 (m, 1H), 3.77 – 3.74 (m, 1H), 3.23 – 3.20 (m, 6H), 2.17 – 2.13 (m, 1H), 1.98 – 1.85 (m, 1H), 1.34 (s, 18H).

***tert*-butyl *N*-[4-[3-(*tert*-butoxycarbonylamino)pyrrolidin-1-yl]-6-fluoro-2-[(oxazole-5-carbonylamino)methyl]-9*H*-pyrimido[4,5-*b*]indol-8-yl]-N-methyl-carbamate (7ad)**

Following the general procedure above: a) *tert*-butyl *N*-[2-(aminomethyl)-4-[3-(*tert*-butoxycarbonylamino)pyrrolidin-1-yl]-6-fluoro-9*H*-pyrimido[4,5-*b*]indol-8-yl]-*N*-methyl-carbamate 200 mg; b) oxazole-5-carboxylic acid 54 mg; c) 94 mg; d) 10 mL; e) 74 µL; f) 90 mg.

Yellow oil; yield 55%; LCMS: R_T = 2.56 min, [M+H]+ 625.6; ^{1}H NMR (400 MHz, CD_3OD) δ_H 8.25 (s, 1H), 7.67 (s, 1H), 7.62 (dd, $^3J_{H\text{-}F}$ = 10.4 Hz, $^4J_{H\text{-}H}$ = 2.3 Hz, 1H), 6.93 (dd, $^3J_{H\text{-}F}$ = 9.8 Hz, $^4J_{H\text{-}H}$ = 2.3 Hz, 1H), 4.52 (s, 2H), 4.13 – 3.93 (m, 3H), 3.92 – 3.81 (m, 2H), 3.74 – 3.67 (m, 1H), 3.19 (s, 3H), 2.21 – 2.07 (m, 1H), 2.00 – 1.83 (m, 1H), 1.33 (s, 18H).

***tert*-butyl *N*-[1-[8-[*tert*-butoxycarbonyl(methyl)amino]-6-fluoro-2-[(oxazole-4-carbonylamino)methyl]-9*H*-pyrimido[4,5-*b*]indol-4-yl]pyrrolidin-3-yl]-*N*-methyl-carbamate (7bc)**

Following the general procedure above: a) *tert*-butyl *N*-[1-[2-(aminomethyl)-8-[*tert*-butoxycarbonyl(methyl)amino]-6-fluoro-9*H*-pyrimido[4,5-*b*]indol-4-yl]pyrrolidin-3-yl]-*N*-methyl-carbamate 48 mg; b) oxazole-4-carboxylic acid 12 mg; c) 18 mg; d) 3 mL; e) 12 µL; f) 30 mg.

Orange solid; yield 53%; LCMS: R_T = 3.49 min, [M+H]+ 639.7.

***tert*-butyl *N*-[1-[8-[*tert*-butoxycarbonyl(methyl)amino]-6-fluoro-2-[(oxazole-5-carbonylamino)methyl]-9*H*-pyrimido[4,5-*b*]indol-4-yl]pyrrolidin-3-yl]-*N*-methyl-carbamate (7bd)**

Following the general procedure above: a) *tert*-butyl *N*-[1-[2-(aminomethyl)-8-[*tert*-butoxycarbonyl(methyl)amino]-6-fluoro-9*H*-pyrimido[4,5-*b*]indol-4-yl]pyrrolidin-3-yl]-*N*-methyl-carbamate 52 mg; b) oxazole-5-carboxylic acid 13 mg; c) 18 mg; d) 4 mL; e) 18 µL; f) 32 mg.

Red film; yield 52%; LCMS: R_T = 3.27 min, [M+H]+ 639.7; ^{1}H NMR (500 MHz, $CDCl_3$) δ_H 9.36 (s, 1H), 8.05 (s, 1H), 7.85 (s, 1H), 7.59 (dd, $^3J_{H\text{-}F}$ = 10.0 Hz, $^4J_{H\text{-}H}$ = 2.2 Hz, 1H), 7.02 – 6.95 (m, 1H), 4.89 – 4.71 (m, 3H), 4.14 – 3.99 (m, 3H), 3.92 (t, *J* = 7.7 Hz, 1H), 3.35 (s, 3H), 2.90 (s, 3H), 2.29 – 2.12 (m, 2H), 1.46 (s, 18H).

***tert*-butyl *N*-[1-[8-[*tert*-butoxycarbonyl(methyl)amino]-6-fluoro-2-[[(4-methyloxazole-5-carbonyl)amino]methyl]-9*H*-pyrimido[4,5-*b*]indol-4-yl]pyrrolidin-3-yl]-*N*-methyl-carbamate (7be)**

Following the general procedure above: a) *tert*-butyl *N*-[1-[2-(aminomethyl)-8-[*tert*-butoxycarbonyl(methyl)amino]-6-fluoro-9*H*-pyrimido[4,5-*b*]indol-4-yl]pyrrolidin-3-yl]-*N*-methyl-carbamate 98 mg; b) 4-methyloxazole-5-carboxylic acid 34 mg; c) 37 mg; d) 6 mL; e) 28 µL; f) 21 mg.

Orange solid; yield 18%; LCMS: R_T = 3.37 min, [M+H]+ 653.3; ^{1}H NMR (500 MHz, $CDCl_3$) δ_H 9.12 (s, 1H), 7.84 (s, 1H), 7.68 (t, *J* = 4.6 Hz, 1H), 7.58 (dd, $^3J_{H\text{-}F}$ = 10.0 Hz, $^4J_{H\text{-}H}$ = 2.2 Hz, 1H), 6.99 (dd, $^3J_{H\text{-}F}$ = 10.0 Hz, $^4J_{H\text{-}H}$ = 2.2 Hz, 1H), 4.69 (d, *J* = 4.6 Hz, 2H), 4.14 – 3.99 (m, 3H), 3.91 (dd, *J* = 10.8, 7.9 Hz, 1H), 3.34 (s, 3H), 2.89 (s, 3H), 2.56 (s, 3H), 2.28 – 2.11 (m, 3H), 1.46 (s, 18H).

***tert*-butyl (4-(3-(dimethylamino)pyrrolidin-1-yl)-6-fluoro-2-((oxazole-5-carboxamido)methyl)-9*H*-pyrimido[4,5-*b*]indol-8-yl)(methyl)carbamate (7cd)**

Following the general procedure above: a) *tert*-butyl *N*-[2-(aminomethyl)-4-[3-(dimethylamino)pyrrolidin-1-yl]-6-fluoro-9*H*-pyrimido[4,5-*b*]indol-8-yl]-*N*-methyl-carbamate 44 mg; b) oxazole-5-carboxylic acid 17 mg; c) 25 mg; d) 5 mL; e) 22 µL; f) 17 mg.

Yellow film; yield 32%; LCMS: R_T = 2.58 min, [M+H]+ 553.2; ^{1}H NMR (500 MHz, $CDCl_3$) δ_H 9.78 (s, 1H), 8.01 (s, 1H), 7.97 (s, 1H), 7.93 (s, 1H), 7.62 (dd, $^3J_{H\text{-}F}$ = 10.2 Hz, $^4J_{H\text{-}H}$ = 2.4 Hz, 1H), 6.98 (dd, $^3J_{H\text{-}F}$ = 10.1 Hz, $^4J_{H\text{-}H}$ = 2.4 Hz, 1H), 4.83 (s, 2H), 4.19 – 4.02 (m, 3H), 3.90 (t, *J* = 9.4 Hz, 1H), 3.35 (s, 3H), 2.84 (m, 1H), 2.39 (s, 6H), 2.33 – 2.28 (m, 1H), 2.02 – 1.98 (m, 1H), 1.43 (s, 9H).

tert-butyl _N_-[4-[3-(dimethylamino)pyrrolidin-1-yl]-6-fluoro-2-[[(4-methyloxazole-5-carbonyl)amino]methyl]-9_H_-pyrimido[4,5-_b_]indol-8-yl]-_N_-methyl-carbamate (7ce)

Following the general procedure above: a) *tert*-butyl *N*-[2-(aminomethyl)-4-[3-(dimethylamino)pyrrolidin-1-yl]-6-fluoro-9*H*-pyrimido[4,5-*b*]indol-8-yl]-*N*-methyl-carbamate 42 mg; b) 4-methyloxazole-5-carboxylic acid 17 mg; c) 24 mg; d) 5 mL; e) 22 µL; f) 20 mg.

Yellow film; yield 38%; LCMS: R_T = 2.53 min, [M+H]+ 567.2; ^{1}H NMR (500 MHz, $CDCl_3$) δ_H 9.04 (s, 1H), 7.84 (s, 1H), 7.74 (t, *J* = 4.6 Hz, 1H), 7.59 (dd, $^3J_{H\text{-}F}$ = 10.0 Hz, $^4J_{H\text{-}H}$ = 2.2 Hz, 1H), 6.97 (dd, $^3J_{H\text{-}F}$ = 9.8 Hz, $^4J_{H\text{-}H}$ = 2.2 Hz, 1H), 4.68 (dd, *J* = 4.6, 2.4 Hz, 2H), 4.15 – 4.01 (m, 3H), 3.96 – 3.89 (m, 1H), 3.33 (s, 3H), 2.85 (s, 1H), 2.56 (s, 3H), 2.43 (s, 6H), 2.35 – 2.29 (m, 1H), 2.04 – 1.99 (m, 1H), 1.44 (s, 9H).

tert-butyl _N_-[4-[3-(dimethylamino)pyrrolidin-1-yl]-6-fluoro-2-[[(2-methyloxazole-5-carbonyl)amino]methyl]-9_H_-pyrimido[4,5-_b_]indol-8-yl]-_N_-methyl-carbamate (7cf)

Following the general procedure above: a) *tert*-butyl *N*-[2-(aminomethyl)-4-[3-(dimethylamino)pyrrolidin-1-yl]-6-fluoro-9*H*-pyrimido[4,5-*b*]indol-8-yl]-*N*-methyl-carbamate 66 mg; b) 2-methyloxazole-5-carboxylic acid 27 mg; c) 38 mg; d) 7 mL; e) 28 µL; f) 42 mg.

Yellow film; yield 51%; LCMS: R_T = 2.64 min, [M+H]+ 567.2.

tert-butyl _N_-[4-[3-(dimethylamino)pyrrolidin-1-yl]-6-fluoro-2-[(furan-2-carbonylamino)methyl]-9_H_-pyrimido[4,5-_b_]indol-8-yl]-_N_-methyl-carbamate (7cg)

Following the general procedure above: a) *tert*-butyl *N*-[2-(aminomethyl)-4-[3-(dimethylamino)pyrrolidin-1-yl]-6-fluoro-9*H*-pyrimido[4,5-*b*]indol-8-yl]-*N*-methyl-carbamate 50 mg; b) furan-2-carboxylic acid 18 mg; c) 27 mg; d) 5 mL; e) 21 µL; f) 28 mg.

Yellow oil; yield 46%; LCMS: R_T = 3.07 min, [M+H]+ 552.4; ^{1}H NMR (500 MHz, $CDCl_3$) δ_H 8.87 (s, 1H), 7.91 – 7.87 (m, 1H), 7.62 (dd, $^3J_{H\text{-}F}$ = 10.1 Hz, $^4J_{H\text{-}H}$ = 2.3 Hz, 1H), 7.50 – 7.45 (m, 1H), 7.19 (d, *J* = 3.5 Hz, 1H), 6.97 (dd, $^3J_{H\text{-}F}$ = 10.0 Hz, $^4J_{H\text{-}H}$ = 2.2 Hz, 1H), 6.53 (dd, *J* = 3.5, 1.6 Hz, 1H), 4.76 – 4.70 (m, 2H), 4.19 – 4.03 (m, 3H), 3.91 – 3.83 (m, 1H), 3.34 (s, 3H), 2.87 – 2.77 (m, 1H), 2.38 (s, 6H), 2.32 – 2.28 (m, 1H), 2.01 – 1.93 (m, 1H), 1.44 (s, 9H).

tert-butyl _N_-[4-[3-(dimethylamino)pyrrolidin-1-yl]-6-fluoro-2-[(1_H_-pyrrolo[2,3-_b_]pyridine-6-carbonylamino)methyl]-9_H_-pyrimido[4,5-_b_]indol-8-yl]-_N_-methyl-carbamate (7ch)

Following the general procedure above: a) *tert*-butyl *N*-[2-(aminomethyl)-4-[3-(dimethylamino)pyrrolidin-1-yl]-6-fluoro-9*H*-pyrimido[4,5-*b*]indol-8-yl]-*N*-methyl-carbamate 42 mg; b) 1*H*-pyrrolo[2,3-*b*]pyridine-6-carboxylic acid 20 mg; c) 22 mg; d) 5 mL; e) 18 µL; f) 11 mg.

Yellow film; yield 21%; LCMS: R_T = 3.46 min, [M+H]+ 602.4

***tert*-butyl *N*-[4-[3-[(*tert*-butoxycarbonylamino)methyl]pyrrolidin-1-yl]-6-fluoro-2-[(oxazole-5-carbonylamino)methyl]-9*H*-pyrimido[4,5-*b*]indol-8-yl]-*N*-methyl-carbamate (7dd)**

Following the general procedure above: a) *tert*-butyl *N*-[2-(aminomethyl)-4-[3-[(*tert*-butoxycarbonylamino)methyl]pyrrolidin-1-yl]-6-fluoro-9*H*-pyrimido[4,5-*b*]indol-8-yl]-*N*-methylcarbamate 60 mg; b) oxazole-5-carboxylic acid 18 mg; c) 29 mg; d) 6 mL; e) 18 µL; f) 47 mg.

Yellow oil; yield 67%; LCMS: R_T = 3.09 min, [M+H]+ 639.2; ^{1}H NMR (500 MHz, $CDCl_3$) δ_H 9.15 (s, 1H), 8.04 (s, 1H), 7.90 (s, 1H), 7.84 (s, 1H), 7.64 (d, $^3J_{H\text{-}F}$ = 9.8 Hz, 1H), 6.97 (dd, $^3J_{H\text{-}F}$ = 9.8 Hz, $^4J_{H\text{-}H}$ = 2.2 Hz, 1H), 4.80 (s, 1H), 4.74 (d, *J* = 4.3 Hz, 2H), 4.10 – 3.97 (m, 2H), 3.76 (t, *J* = 9.1 Hz, 1H), 3.34 (s, 3H), 3.32 – 3.20 (m, 2H), 2.63 – 2.49 (m, 1H), 2.25 – 2.14 (m, 1H), 1.89 – 1.78 (m, 1H), 1.44 (s, 18H).

tert-butyl *N*-[4-[3-[(*tert*-butoxycarbonylamino)methyl]pyrrolidin-1-yl]-6-fluoro-2-[[(4-methyloxazole-5-carbonyl)amino]methyl]-9*H*-pyrimido[4,5-*b*]indol-8-yl]-*N*-methyl-carbamate (7de)

Following the general procedure above: a) *tert*-butyl *N*-[2-(aminomethyl)-4-[3-[(*tert*-butoxycarbonylamino)methyl]pyrrolidin-1-yl]-6-fluoro-9*H*-pyrimido[4,5-*b*]indol-8-yl]-*N*-methylcarbamate 59 mg; b) 4-methyloxazole-5-carboxylic acid 20 mg; c) 28 mg; d) 6 mL; e) 19 µL; f) 29 mg.

Yellow oil; yield 36%; LCMS: R_T = 3.24 min, [M+H]+ 653.3; ^{1}H NMR (500 MHz, $CDCl_3$) δ_H 8.65 (s, 1H), 7.87 (s, 1H), 7.76 (s, 1H), 7.64 (d, $^3J_{H\text{-}F}$ = 9.8 Hz, 1H), 6.97 (dd, $^3J_{H\text{-}F}$ = 9.7 Hz, $^4J_{H\text{-}H}$ = 2.2 Hz, 1H), 4.79 – 4.71 (m, 1H), 4.67 (d, *J* = 4.5 Hz, 2H), 4.09 – 4.01 (m, 2H), 3.75 (t, *J* = 9.2 Hz, 1H), 3.34 (s, 3H), 3.31 – 3.22 (m, 2H), 2.57 (s, 3H), 2.61 – 2.49 (m, 1H), 2.24 – 2.15 (m, 1H), 1.87 – 1.77 (m, 1H), 1.44 (s, 18H).

tert-butyl *N*-[4-[3-[(*tert*-butoxycarbonylamino)methyl]pyrrolidin-1-yl]-6-fluoro-2-[[(2-methyloxazole-5-carbonyl)amino]methyl]-9*H*-pyrimido[4,5-*b*]indol-8-yl]-*N*-methyl-carbamate (7df)

Following the general procedure above: a) *tert*-butyl *N*-[2-(aminomethyl)-4-[3-[(*tert*-butoxycarbonylamino)methyl]pyrrolidin-1-yl]-6-fluoro-9*H*-pyrimido[4,5-*b*]indol-8-yl]-*N*-methylcarbamate 59 mg; b) 2-methyloxazole-5-carboxylic acid 20 mg; c) 28 mg; d) 6 mL; e) 20 µL; f) 24 mg.

Yellow oil; yield 36%; LCMS: R_T = 3.21 min, [M+H]+ 653.2; ^{1}H NMR (500 MHz, $CDCl_3$) δ_H 8.94 (s, 1H), 7.74 (s, 1H), 7.64 (m, 2H), 7.01 – 6.92 (m, 1H), 4.81 (s, 1H), 4.71 (d, *J* = 4.4 Hz, 2H), 4.10 – 3.96 (m, 2H), 3.77 (t, *J* = 9.1 Hz, 1H), 3.34 (s, 3H), 3.32 – 3.20 (m, 2H), 2.57 (s, 3H), 2.24 – 2.14 (m, 1H), 1.88 – 1.79 (m, 1H), 1.70 – 1.61 (m, 1H), 1.44 (s, 18H).

methyl 6-[[4-[3-[(*tert*-butoxycarbonylamino)methyl]pyrrolidin-1-yl]-8-[*tert*-butoxycarbonyl(methyl)amino]-6-fluoro-9*H*-pyrimido[4,5-*b*]indol-2-yl]methylcarbamoyl]pyridine-2-carboxylate (7di)

Following the general procedure above: a) *tert*-butyl *N*-[2-(aminomethyl)-4-[3-[(*tert*-butoxycarbonylamino)methyl]pyrrolidin-1-yl]-6-fluoro-9*H*-pyrimido[4,5-*b*]indol-8-yl]-*N*-methylcarbamate 55 mg; b) 6-methoxycarbonylpyridine-2-carboxylic acid 25 mg; c) 24 mg; d) 6 mL; e) 21 µL; f) 34 mg.

Yellow oil; yield 52%; LCMS: R_T = 3.59 mins, [M+H]+ 707.2; ^{1}H NMR (500 MHz, $CDCl_3$) δ_H 9.53 – 9.41 (m, 1H), 8.94 (s, 1H), 8.49 (d, *J* = 7.7 Hz, 1H), 8.23 (dd, *J* = 7.6 Hz, $^4J_{H\text{-}H}$ = 1.2 Hz, 1H), 8.04 (t, *J* = 7.8 Hz, 1H), 7.64 (d, $^3J_{H\text{-}F}$ = 9.6 Hz, 1H), 6.96 (dd, $^3J_{H\text{-}F}$ = 9.8 Hz, $^4J_{H\text{-}H}$ = 2.2 Hz, 1H), 5.37 – 5.28 (m, 1H), 4.83 (d,

J = 4.6 Hz, 2H), 4.23 – 4.16 (m, 2H), 4.05 (s, 3H), 3.91 – 3.83 (m, 1H), 3.39 – 3.26 (m, 5H), 2.65 – 2.56 (m, 1H), 2.24 – 2.17 (m, 1H), 1.91 – 1.82 (m, 1H), 1.46 – 1.39 (m, 18H).

General procedure for Boc deprotection to yield final target compounds (2)

Following the general procedure below, the data are reported as a) mass of starting material; b) volume of MeOH; c) volume of HCl (4M in dioxane); d) mass of product obtained as the HCl salt.

To a solution of corresponding Boc-protected compound **7** (0.006 - 0.06 mmol) in MeOH was added HCl (4 M in dioxane) (0.01 – 6.30 mmol). The reaction mixture was stirred at RT for 30 min then concentrated *in vacuo* and azeotroped from MeOH twice to give the corresponding Boc-deprotected final compound **2** in good yield.

2-(aminomethyl)-4-(3-aminopyrrolidin-1-yl)-6-fluoro-*N*-methyl-9*H*-pyrimido[4,5-*b*]indol-8-amine hydrochloride (8)

Following the general procedure above: a) *tert*-butyl *N*-[1-[2-(aminomethyl)-8-[*tert*-butoxycarbonyl(methyl)amino]-6-fluoro-9*H*-pyrimido[4,5-*b*]indol-4-yl]pyrrolidin-3-yl]-*N*-methyl-carbamate 15 mg; b) 1.5 mL; c) 1.5 mL; d) 6 mg.

Yellow solid; yield 52%; LCMS: R_T = 1.68 min, [M+H]+ 330.5.

***N*-[[4-(3-aminopyrrolidin-1-yl)-6-fluoro-8-(methylamino)-9*H*-pyrimido[4,5-*b*]indol-2-yl]methyl]pyridine-3-carboxamide hydrochloride (2aa)**

Following the general procedure above: a) *tert*-butyl *N*-[4-[3-(*tert*-butoxycarbonylamino)pyrrolidin-1-yl]-6-fluoro-2-[(pyridine-3-carbonylamino)methyl]-9*H*-pyrimido[4,5-*b*]indol-8-yl]-*N*-methyl-carbamate 6 mg; b) 1.2 mL; c) 1.2 mL; d) 6 mg.

Yellow solid; yield quant.; LCMS: R_T = 1.72 min, [M+H]+ 435.4.

***N*-[[4-(3-aminopyrrolidin-1-yl)-6-fluoro-8-(methylamino)-9*H*-pyrimido[4,5-*b*]indol-2-yl]methyl]pyridazine-3-carboxamide hydrochloride (2ab)**

Following the general procedure above: a) *tert*-butyl *N*-[4-[3-(*tert*-butoxycarbonylamino)pyrrolidin-1-yl]-6-fluoro-2-[(pyridazine-3-carbonylamino)methyl]-9*H*-pyrimido[4,5-*b*]indol-8-yl]-*N*-methyl-carbamate 4 mg; b) 1.2 mL; c) 1.2 mL; d) 3 mg.

Yellow solid; yield 94%; LCMS: R_T = 1.79 min, [M+H]+ 436.5.

***N*-[[4-(3-aminopyrrolidin-1-yl)-6-fluoro-8-(methylamino)-9*H*-pyrimido[4,5-*b*]indol-2-yl]methyl]oxazole-4-carboxamide hydrochloride (2ac)**

Following the general procedure above: a) *tert*-butyl *N*-[4-[3-(tert-butoxycarbonylamino)pyrrolidin-1-yl]-6-fluoro-2-[(oxazole-4-carbonylamino)methyl]-9*H*-pyrimido[4,5-*b*]indol-8-yl]-*N*-methyl-carbamate 22 mg; b) 2.5 mL; c) 2.5 mL; d) 15 mg.

Yellow solid; yield 98%; LCMS: R_T = 1.80 min, [M+H]+ 426.5; ^{1}H NMR (400 MHz, DMSO-d_6) δ_H 12.50 (s, 1H), 8.70 (d, $^4J_{H\text{-}H}$ = 1.0 Hz, 1H), 8.58 (d, $^4J_{H\text{-}H}$ = 1.0 Hz, 1H), 7.08 (dd, $^3J_{H\text{-}F}$ = 11.1 Hz, $^4J_{H\text{-}H}$ = 2.2 Hz, 1H), 6.39 (dd, $^3J_{H\text{-}F}$ = 12.0 Hz, $^4J_{H\text{-}H}$ = 2.2 Hz, 1H), 4.62 (s, 2H), 4.29 – 4.17 (m, 2H), 4.08 – 3.95 (m, 3H), 2.87 (s, 3H), 2.40 – 2.27 (m, 1H), 2.27 – 2.19 (m, 1H).

_N_-[[4-(3-aminopyrrolidin-1-yl)-6-fluoro-8-(methylamino)-9_H_-pyrimido[4,5-_b_]indol-2-yl]methyl]oxazole-5-carboxamide hydrochloride (2ad)

Following the general procedure above: a) *tert*-butyl *N*-[4-[3-(*tert*-butoxycarbonylamino)pyrrolidin-1-yl]-6-fluoro-2-[(oxazole-5-carbonylamino)methyl]-9*H*-pyrimido[4,5-*b*]indol-8-yl]-N-methyl-carbamate 90 mg; b) 2 mL; c) 4 mL; d) 60 mg.

Yellow solid; yield 98%; LCMS: R_T = 2.17 min, [M+H]+ 425.2; ^{1}H NMR (400 MHz, DMSO-d_6) δ_H 12.10 (s, 1H), 9.12 (t, *J* = 6.0 Hz, 1H), 8.66 (s, 1H), 8.37 (s, 2H), 7.94 (s, 1H), 7.12 (dd, $^3J_{H\text{-}F}$ = 11.1 Hz, $^4J_{H\text{-}H}$ = 2.2 Hz, 1H), 6.42 (dd, $^3J_{H\text{-}F}$ = 12.0 Hz, $^4J_{H\text{-}H}$ = 2.2 Hz, 1H), 4.61 (d, *J* = 6.0 Hz, 2H), 4.26 – 4.18 (m, 2H), 4.06 – 3.99 (m, 3H), 2.92 (s, 3H), 2.39 – 2.33 (m, 1H), 2.25 – 2.16 (m, 1H).

_N_-[[6-fluoro-8-(methylamino)-4-[3-(methylamino)pyrrolidin-1-yl]-9_H_-pyrimido[4,5-_b_]indol-2-yl]methyl]oxazole-4-carboxamide hydrochloride (2bc)

Following the general procedure above: a) *tert*-butyl *N*-[1-[8-[*tert*-butoxycarbonyl(methyl)amino]-6-fluoro-2-[(oxazole-4-carbonylamino)methyl]-9*H*-pyrimido[4,5-*b*]indol-4-yl]pyrrolidin-3-yl]-*N*-methyl-carbamate 30 mg; b) 4 mL; c) 0.1 mL; d) 3 mg.

White solid; yield 14%; LCMS: R_T = 2.33 min, [M+H]+ 439.1; ^{1}H NMR (500 MHz, DMSO-d_6) δ_H 11.67 (s, 1H), 8.69 (d, $^4J_{H\text{-}H}$ = 1.1 Hz, 1H), 8.56 (d, $^4J_{H\text{-}H}$ = 1.1 Hz, 1H), 8.52 (t, *J* = 5.4 Hz, 1H), 7.04 (dd, $^3J_{H\text{-}F}$ = 11.1 Hz, $^4J_{H\text{-}H}$ = 2.2 Hz, 1H), 6.30 (dd, $^3J_{H\text{-}F}$ = 11.8 Hz, $^4J_{H\text{-}H}$ = 2.2 Hz, 1H), 5.73 (d, *J* = 5.0 Hz, 1H), 4.47 (d, *J* = 5.5 Hz, 2H), 4.02 – 3.92 (m, 2H), 3.87 – 3.79 (m, 1H), 3.64 (dd, *J* = 10.7, 4.3 Hz, 1H), 3.27 – 3.23 (m, 1H), 2.86 (d, *J* = 4.9 Hz, 3H), 2.28 (s, 3H), 2.07 – 2.00 (m, 1H), 1.87 – 1.80 (m, 1H).

_N_-[[6-fluoro-8-(methylamino)-4-[3-(methylamino)pyrrolidin-1-yl]-9_H_-pyrimido[4,5-_b_]indol-2-yl]methyl]oxazole-5-carboxamide hydrochloride (2bd)

Following the general procedure above: a) *tert*-butyl *N*-[1-[8-[*tert*-butoxycarbonyl(methyl)amino]-6-fluoro-2-[(oxazole-5-carbonylamino)methyl]-9*H*-pyrimido[4,5-*b*]indol-4-yl]pyrrolidin-3-yl]-*N*-methyl-carbamate 32 mg; b) 5 mL; c) 0.1 mL; d) 7 mg.

Beige solid; yield 32%; LCMS: R_T = 2.33 min, [M+H]+ 439.4; ^{1}H NMR (500 MHz, DMSO-d_6) δ_H 11.59 (s, 1H), 8.95 (t, *J* = 6.0 Hz, 1H), 8.59 (s, 1H), 7.85 (s, 1H), 7.03 (dd, $^3J_{H\text{-}F}$ = 11.1 Hz, $^4J_{H\text{-}H}$ = 2.2 Hz, 1H), 6.31 (dd, $^3J_{H\text{-}F}$ = 12.0 Hz, $^4J_{H\text{-}H}$ = 2.2 Hz, 1H), 5.66 (d, *J* = 5.0 Hz, 1H), 4.47 (d, *J* = 6.0 Hz, 2H), 4.04 – 3.93 (m, 2H), 3.87 – 3.79 (m, 1H), 3.71 (dd, *J* = 11.1, 4.3 Hz, 1H), 3.44 – 3.40 (m, 1H), 2.85 (d, *J* = 5.0 Hz, 3H), 2.38 (s, 3H), 2.15 – 2.07 (m, 1H), 1.96 – 1.89 (m, 1H).

_N_-((6-fluoro-8-(methylamino)-4-(3-(methylamino)pyrrolidin-1-yl)-9_H_-pyrimido[4,5-_b_]indol-2-yl)methyl)-4-methyloxazole-5-carboxamide hydrochloride (2be)

Following the general procedure above: a) *tert*-butyl *N*-[1-[8-[*tert*-butoxycarbonyl(methyl)amino]-6-fluoro-2-[[(4-methyloxazole-5-carbonyl)amino]methyl]-9*H*-pyrimido[4,5-*b*]indol-4-yl]pyrrolidin-3-yl]-*N*-methyl-carbamate 21 mg; b) 3 mL; c) 0.1 mL; d) 15 mg.

Orange solid; yield 93%; LCMS: R_T = 2.37 min, [M+H]+ 453.1; ^{1}H NMR (500 MHz, DMSO-d_6) δ_H 12.42 (s, 1H), 9.16 – 9.00 (m, 2H), 8.87 (t, *J* = 7.1 Hz, 1 H), 8.47 (s, 1H), 7.07 (dd, $^3J_{H\text{-}F}$ = 10.7 Hz, $^4J_{H\text{-}H}$ = 2.2 Hz, 1H), 6.40 (dd, $^3J_{H\text{-}F}$ = 11.4 Hz, $^4J_{H\text{-}H}$ 2.2 Hz, 1H), 4.59 (d, *J* = 5.9 Hz, 2H), 4.29 – 4.16 (m, 2H), 4.15 – 4.05 (m, 1H), 4.04 – 3.97 (m, 1H), 3.97 – 3.87 (m, 1H), 2.86 (s, 3H), 2.64 (s, 3H), 2.56 – 2.51 (m, 1H), 2.38 (s, 3H), 2.36 – 2.35 (m, 1H).

_N_-[[4-[3-(dimethylamino)pyrrolidin-1-yl]-6-fluoro-8-(methylamino)-9_H_-pyrimido[4,5-_b_]indol-2-yl]methyl]oxazole-5-carboxamide hydrochloride (2cd)

Following the general procedure above: a) *tert*-butyl (4-(3-(dimethylamino)pyrrolidin-1-yl)-6-fluoro-2-((oxazole-5-carboxamido)methyl)-9*H*-pyrimido[4,5-*b*]indol-8-yl)(methyl)carbamate 17 mg; b) 1 mL; c) 0.1 mL; d) 7 mg.

Yellow solid; yield 32%; LCMS: R_T = 2.34 min, [M+H]+ 453.1; ^{1}H NMR (500 MHz, DMSO-d_6) δ_H 12.32 (s, 1H), 10.59 (s, 1H), 9.19 (t, *J* = 6.0 Hz, 1H), 8.60 (s, 1H), 7.88 (s, 1H), 7.07 (dd, $^3J_{H\text{-}F}$ = 10.7 Hz, $^4J_{H\text{-}H}$ = 2.2 Hz, 1H), 6.40 (dd, $^3J_{H\text{-}F}$ = 11.9 Hz, $^4J_{H\text{-}H}$ = 2.2 Hz, 1H), 4.61 (d, *J* = 6.1 Hz, 2H), 4.27 – 4.11 (m, 3H), 4.13 – 3.98 (m, 2H), 2.86 (s, 3H), 2.84 (d, *J* = 11.6 Hz, 6H), 2.55 – 2.52 (m, 1H), 2.35 – 2.25 (m, 1H).

_N_-[[4-[3-(dimethylamino)pyrrolidin-1-yl]-6-fluoro-8-(methylamino)-9_H_-pyrimido[4,5-_b_]indol-2-yl]methyl]-4-methyl-oxazole-5-carboxamide hydrochloride (2ce)

Following the general procedure above: a) *tert*-butyl *N*-[4-[3-(dimethylamino)pyrrolidin-1-yl]-6-fluoro-2-[[(4-methyloxazole-5-carbonyl)amino]methyl]-9*H*-pyrimido[4,5-*b*]indol-8-yl]-*N*-methyl-carbamate 20 mg; b) 1 mL; c) 0.1 mL; d) 14 mg.

Orange solid; yield 85%; LCMS: R_T = 2.46 min, [M+H]+ 467.1; ^{1}H NMR (500 MHz, DMSO-d_6) δ_H 12.40 (s, 1H), 10.72 (s, 1H), 8.86 (s, 1H), 8.46 (s, 1H), 7.06 (d, $^3J_{H\text{-}F}$ = 10.7 Hz, 1H), 6.40 (d, $^3J_{H\text{-}F}$ = 11.7 Hz, 1H), 4.59 (d, *J* = 5.8 Hz, 2H), 4.29 – 4.13 (m, 3H), 4.12 – 3.96 (m, 2H), 2.88 – 2.78 (m, 9H), 2.64 – 2.60 (m, 1H), 2.37 (s, 3H), 2.37 – 2.33 (m, 1H).

_N_-[[4-[3-(dimethylamino)pyrrolidin-1-yl]-6-fluoro-8-(methylamino)-9_H_-pyrimido[4,5-_b_]indol-2-yl]methyl]-2-methyl-oxazole-5-carboxamide hydrochloride (2cf)

Following the general procedure above: a) *tert*-butyl *N*-[4-[3-(dimethylamino)pyrrolidin-1-yl]-6-fluoro-2-[[(2-methyloxazole-5-carbonyl)amino]methyl]-9*H*-pyrimido[4,5-*b*]indol-8-yl]-*N*-methyl-carbamate 42 mg; b) 2 mL; c) 0.2 mL; d) 7 mg.

Beige solid; yield 32%; LCMS: R_T = 2.35 min, [M+H]+ 467.2; ^{1}H NMR (500 MHz, DMSO-d_6) δ_H 12.47 (s, 1H), 10.41 (s, 1H), 9.11 (t, *J* = 6.0 Hz, 1H), 7.73 (s, 1H), 7.09 (dd, $^3J_{H\text{-}F}$ = 10.7 Hz, $^4J_{H\text{-}H}$ = 2.2 Hz, 1H), 6.42 (dd, $^3J_{H\text{-}F}$ = 12.0 Hz, $^4J_{H\text{-}H}$ = 2.2 Hz, 1H), 4.62 (d, *J* = 6.0 Hz, 2H), 4.29 – 3.98 (m, 5H), 2.89 – 2.82 (m, 9H), 2.75 (t, *J* = 5.1 Hz, 1H), 2.47 – 2.43 (m, 3H), 2.34 – 2.28 (m, 1H).

_N_-[[4-[3-(dimethylamino)pyrrolidin-1-yl]-6-fluoro-8-(methylamino)-9_H_-pyrimido[4,5-_b_]indol-2-yl]methyl]furan-2-carboxamide (2cg)

Following the general procedure above: a) *tert*-butyl *N*-[4-[3-(dimethylamino)pyrrolidin-1-yl]-6-fluoro-2-[(furan-2-carbonylamino)methyl]-9*H*-pyrimido[4,5-*b*]indol-8-yl]-*N*-methyl-carbamate 28 mg; b) 2 mL; c) 0.2 mL; d) 11 mg.

Yellow solid; yield 48%; LCMS: R_T = 2.80 min, [M+H]+ 452.3; ^{1}H NMR (500 MHz, DMSO-d_6) δ_H 12.45 (s, 1H), 11.38 (s, 1H), 8.89 (t, *J* = 5.9 Hz, 1H), 7.92 – 7.88 (m, 1H), 7.25 – 7.20 (m, 1H), 7.05 (dd, $^3J_{H\text{-}F}$ = 11.0 Hz, $^4J_{H\text{-}H}$ = 2.2 Hz, 1H), 6.70 – 6.65 (m, 1H), 6.39 (dd, $^3J_{H\text{-}F}$ = 11.9 Hz, $^4J_{H\text{-}H}$ = 2.1 Hz, 1H), 4.62 – 4.57 (m, 2H), 4.23 – 4.16 (m, 3H), 4.10 – 3.96 (m, 2H), 2.86 (s, 3H), 2.81 (dd, *J* = 18.3, 4.7 Hz, 6H), 2.47 – 2.43 (m, 1H), 2.41 – 2.32 (m, 1H).

_N_-[[4-[3-(dimethylamino)pyrrolidin-1-yl]-6-fluoro-8-(methylamino)-9_H_-pyrimido[4,5-_b_]indol-2-yl]methyl]-1_H_-pyrrolo[2,3-_b_]pyridine-6-carboxamide hydrochloride (2ch)

Following the general procedure above: a) *tert*-butyl *N*-[4-[3-(dimethylamino)pyrrolidin-1-yl]-6-fluoro-2-[(1*H*-pyrrolo[2,3-*b*]pyridine-6-carbonylamino)methyl]-9*H*-pyrimido[4,5-*b*]indol-8-yl]-*N*-methyl-carbamate 11 mg; b) 1 mL; c) 0.1 mL; d) 9 mg.

Yellow solid; yield 98%; LCMS: R_T = 3.21 min, [M+H]+ 502.3; ^{1}H NMR (500 MHz, DMSO-d_6) δ_H 12.31 (s, 1H), 11.91 (s, 1H), 10.63 (s, 1H), 9.06 (t, *J* = 5.7 Hz, 1H), 8.14 (d, *J* = 8.1 Hz, 1H), 7.86 (d, *J* = 8.1 Hz, 1H), 7.75 – 7.71 (m, 1H), 7.08 (dd, $^3J_{H\text{-}F}$ = 10.9 Hz, $^4J_{H\text{-}H}$ = 2.2 Hz, 1H), 6.60 (dd, *J* = 3.4, 1.8 Hz, 1H), 6.41 (dd, $^3J_{H\text{-}F}$ = 12.0 Hz, $^4J_{H\text{-}H}$ = 2.2 Hz, 1H), 4.75 (d, *J* = 5.7 Hz, 2H), 4.29 – 4.15 (m, 3H), 4.14 – 4.06 (m, 1H), 4.05 – 3.98 (m, 1H), 2.87 (s, 3H), 2.87 – 2.73 (m, 6H), 2.47 – 2.45 (m, 1H), 2.36 – 2.28 (m, 1H).

_N_-[[4-[3-(aminomethyl)pyrrolidin-1-yl]-6-fluoro-8-(methylamino)-9_H_-pyrimido[4,5-_b_]indol-2-yl]methyl]oxazole-5-carboxamide hydrochloride (2dd)

Following the general procedure above: a) *tert*-butyl *N*-[4-[3-[(*tert*-butoxycarbonylamino)methyl]pyrrolidin-1-yl]-6-fluoro-2-[(oxazole-5-carbonylamino)methyl]-9*H*-pyrimido[4,5-*b*]indol-8-yl]-*N*-methyl-carbamate 47 mg; b) 2 mL; c) 0.2 mL; d) 7 mg.

Yellow solid; yield 32%; LCMS: R_T = 2.13 min, [M+H]+ 439.1; ^{1}H NMR (500 MHz, CD_3OD) δ_H 8.32 (s, 1H), 7.75 (s, 1H), 7.13 (dd, $^3J_{H\text{-}F}$ = 10.7 Hz, $^4J_{H\text{-}H}$ = 2.2 Hz, 1H), 6.43 (dd, $^3J_{H\text{-}F}$ = 10.7 Hz, $^4J_{H\text{-}H}$ = 2.2 Hz, 1H), 4.68 (s, 2H), 4.28 – 4.19 (m, 1H), 4.15 – 4.05 (m, 2H), 3.88 – 3.79 (m, 1H), 3.15 – 3.08 (m, 2H), 3.05 – 2.99 (m, 1H), 2.88 (s, 3H), 2.70 – 2.62 (m, 1H), 2.35 – 2.27 (m, 1H), 1.90 – 1.83 (m, 1H).

_N_-[[4-[3-(aminomethyl)pyrrolidin-1-yl]-6-fluoro-8-(methylamino)-9_H_-pyrimido[4,5-_b_]indol-2-yl]methyl]-4-methyl-oxazole-5-carboxamide hydrochloride (2de)

Following the general procedure above: a) *tert*-butyl *N*-[4-[3-[(*tert*-butoxycarbonylamino)methyl]pyrrolidin-1-yl]-6-fluoro-2-[[(4-methyloxazole-5-carbonyl)amino]methyl]-9*H*-pyrimido[4,5-*b*]indol-8-yl]-*N*-methyl-carbamate 29 mg; b) 2 mL; c) 0.2 mL; d) 21 mg.

Yellow solid; yield 99%; LCMS: R_T = 2.26 min, [M+H]+ 453.1; ^{1}H NMR (500 MHz, CD_3OD) δ_H 8.19 (s, 1H), 7.14 (d, $^3J_{H\text{-}F}$ = 10.5 Hz, 1H), 6.44 (d, $^3J_{H\text{-}F}$ = 10.5 Hz, 1H), 4.65 (s, 2H), 4.33 – 4.19 (m, 1H), 4.19 – 4.04 (m, 2H), 3.92 – 3.79 (m, 1H), 3.09 – 2.96 (m, 2H), 2.88 (s, 3H), 2.74 – 2.64 (m, 1H), 2.38 (s, 3H), 2.35 – 2.28 (m, 1H), 1.96 – 1.84 (m, 1H).

_N_-[[4-[3-(aminomethyl)pyrrolidin-1-yl]-6-fluoro-8-(methylamino)-9_H_-pyrimido[4,5-_b_]indol-2-yl]methyl]-2-methyl-oxazole-5-carboxamide hydrochloride (2df)

Following the general procedure above: a) *tert*-butyl *N*-[4-[3-[(*tert*-butoxycarbonylamino)methyl]pyrrolidin-1-yl]-6-fluoro-2-[[(2-methyloxazole-5-carbonyl)amino]methyl]-9*H*-pyrimido[4,5-*b*]indol-8-yl]-*N*-methyl-carbamate 24 mg; b) 2 mL; c) 0.2 mL; d) 14 mg.

Yellow solid; yield 84%; LCMS: R_T = 2.30 min, [M+H]+ 453.3; ^{1}H NMR (500 MHz, CD_3OD) δ_H 7.61 (s, 1H), 7.11 (dd, $^3J_{H\text{-}F}$ = 11.0 Hz, $^4J_{H\text{-}H}$ = 2.2 Hz, 1H), 6.41 (dd, $^3J_{H\text{-}F}$ = 11.0 Hz, $^4J_{H\text{-}H}$ = 2.2 Hz, 1H), 4.65 (s, 2H), 4.28 – 4.19 (m, 1H), 4.18 – 4.01 (m, 2H), 3.89 – 3.77 (m, 1H), 3.14 – 3.09 (m, 2H), 3.06 – 2.99 (m, 2H), 2.87 (s, 3H), 2.70 – 2.60 (m, 1H), 2.47 (s, 3H), 2.36 – 2.26 (m, 1H), 1.95 – 1.80 (m, 1H).

methyl 6-[[4-[3-(aminomethyl)pyrrolidin-1-yl]-6-fluoro-8-(methylamino)-9*H*-pyrimido[4,5-*b*]indol-2-yl]methylcarbamoyl]pyridine-2-carboxylate hydrochloride (2di)

Following the general procedure above: a) methyl 6-[[4-[3-[(*tert*-butoxycarbonylamino)methyl]pyrrolidin-1-yl]-8-[*tert*-butoxycarbonyl(methyl)amino]-6-fluoro-9*H*-pyrimido[4,5-*b*]indol-2-yl]methylcarbamoyl]pyridine-2-carboxylate 34 mg; b) 1 mL; c) 0.1 mL; d) 21 mg.

Orange solid; yield 86%; LCMS: R_T = 2.65 mins, [M+H]+ 507.1; ^{1}H NMR (500 MHz, CD_3OD) δ_H 8.29 – 8.23 (m, 2H), 8.12 (t, *J* = 7.9 Hz, 1H), 7.09 (dd, $^3J_{H\text{-}F}$ = 10.4 Hz, $^4J_{H\text{-}H}$ = 2.2 Hz, 1H), 6.38 (dd, $^3J_{H\text{-}F}$ = 11.7 Hz, $^4J_{H\text{-}H}$ = 2.2 Hz, 1H), 4.77 – 4.76 (m, 2H), 4.31 – 4.21 (m, 1H), 4.19 – 4.04 (m, 2H), 3.96 (s, 3H), 3.89 – 3.81 (m, 1H), 3.16 – 3.11 (m, 1H), 3.06 – 2.99 (m, 1H), 2.86 (s, 3H), 2.70 – 2.61 (m, 1H), 2.35 – 2.27 (m, 1H), 1.93 – 1.81 (m, 1H).